ELECTRO DYNAMIC SORTING OF METALS, ALLOYS

AND SCRAP

by

Nakul Dholu

A thesis submitted to the faculty of
The University of Utah
in partial fulfillment of the requirements for the degree of

Master of Science

Department of Metallurgical Engineering

The University of Utah

May 2016

The University of Utah Graduate School

STATEMENT OF THESIS APPROVAL

The thesis of   **Nakul Dholu**

has been approved by the following supervisory committee members:

Raj K. Rajamani	, Chair	**2/24/2016**
		Date Approved
Manoranjan Misra	, Member	**2/24/2016**
		Date Approved
Swomitra Kumar Mohanty	, Member	**2/24/2016**
		Date Approved

and by   **Manoranjan Misra**   , Chair/Dean of

the Department/College/School of   **Metallurgical Engineering**

and by David B. Kieda, Dean of The Graduate School.

ABSTRACT

Magnetic separation technology has been utilized for many years in the scrap sorting industry. Ferrous metal scrap is easily sorted using magnetic separation while sorting nonferrous scrap is a tricky process. Currently available technology to sort nonferrous material using mechanical eddy current sorters have limitations in terms of the capability to sort material larger than a quarter inch. Moving parts are subjected to wear and tear and they are also incapable of sorting different nonferrous metals and alloys like aluminum, aluminum alloys, copper, copper alloys, titanium, and so forth, from one another.

The research work presented in this thesis reveals various nonferrous metals and alloy sorting test results using solid state, variable-frequency eddy current technology. The setup for this technology consists of a ferrite core with a V-shaped cut for the air gap wound with wire to produce an alternating magnetic field in the gap when supplied with alternating current. Nonferrous particles, when fed into the gap, interact with the external magnetic field which induces eddy currents into the material, and based on Lenz's law, material tends to deflect away from the source of external magnetic field.

Frequency determination for the selective sorting of material from the mixture of nonferrous material was done based on the ejection velocity experiments performed on size, ranging 4mm to 12mm at a frequency range of 1kHz - 8 kHz on aluminum, copper, brass, and titanium. Ejection velocity results were used to determine an optimal strategy

and sorting experiments of nonferrous metals and alloy mixtures were conducted using a double stacked core of ferrite material having a 2mm inner gap and 33 mm outer gap. Also, experiments were conducted to sort zorba scrap using a larger size NiZn ferrite core with a 10mm inner gap and 20 mm outer gap.

The pendulum experiment showed a trend of increasing ejection velocity with respect to increasing frequency, but the magnitude of velocity for different materials differ at a particular frequency is not the same, this allowed for an optimal frequency to be determined for optimal sorting. Nonferrous materials were sorted very well using both single and double stacked ferrite cores, but grade and recovery was slightly better when the double core was used. Promising results were also achieved for aluminum alloy sorting. All the results strongly indicate that capability for the solid state eddy current sorting technique is to be used to sort various nonferrous metals and alloys when operated at the optimal frequency.

To my parents, fiancée, brother and sister

TABLE OF CONTENTS

LIST OF TABLES

LIST OF FIGURES

ACKNOWLEDGEMENTS

I would like to acknowledge Dr. Raj K. Rajamani for all the guidance and encouragement he gave me in every aspect during the research which led to the successful completion of it. I am also thankful to my Supervisory Committee members, Dr. Manoranjan Misra and Dr. Swomita Kumar Mohanty for their support and interest in my research work.

I would like to thank the following individuals for their contributions: James Nagel, David Cohrs, and Jake Salgado the moral and technical support and for being companions in my time of need.

I would like to acknowledge the Advance Research Project Agency- Energy (ARPA-E) for the financial support of this research project.

Finally, I would like to thank my parents, fiancée, brother, and sister for providing me moral support throughout the whole course of my research work.

CHAPTER 1

INTRODUCTION

Metals play a key role in economic development and they are the backbone of the manufacturing industry. For years, various metals have been extracted from the mineral ore found in nature, but with time high grade ore is getting depleted and the option we are left with is to process low grade ore, which makes recovery process expensive. In such a scenario, recycling metals seems a lucrative option as it is beneficial to the environment by reducing the amount of scrap or waste material being sent to landfills.

Typical sources of scrap come from end-of-life products like autos, household equipment such as washing machines and refrigerators, electronic components, and waste products generated during the manufacturing process. The scrap constitutes a mixture of ferrous, nonferrous, semiconductors, plastic, glass, and rubber fragments. If the mixture of scrap is sorted to streams of similar material fractions, then its monetary value increases compared to the value of unsorted scrap. To do so the scrap is processed in various sorting operations. Initially, the ferrous materials fraction is sorted out using a magnetic separation process and the unsorted scrap is then processed with a mechanical eddy current sorter and other concentrating techniques to separate nonferrous scrap fractions from nonmetallic scrap fractions. The sorted nonferrous material fraction is termed "zorba," and is composed of aluminum, copper, brass, and lead. Sorted aluminum

 fractions from zorba is called "twitch," and due to the higher concentration of aluminum purity in twitch, it has more economic value compared to aluminum sold as zorba. Further economic value additions to twitch can be achieved if it is sorted based on different alloy fractions like common cast alloy, that is, 3XX series and wrought alloys, that is, 1XXX – 7XXX series. Sorted twitch adds 50% economic value which is around 90% of the price of the pure aluminum metal, than compared to twitch if sold unsorted (*1*).

Electro winning and pyrometallurgical techniques can be used to sort zorba, but they are high energy intensive operations. Aluminum extraction consumes 49×10^6 J/kg of aluminum recovered and copper recovery from the smelting operation consumes 50×10^6 J/kg of copper recovered (*2*). Hand picking or manual sorting can be utilized to sort zorba, but it is a slow, high labor intensive operation. Further, it is impossible to separate optically indistinguishable materials (*3*). Sink-float or dense media separation process can sort heavy material form light material, but it is difficult to sort twitch by this process due to a lower difference in density. Moreover, large amounts of water is required for the operation along with chemical additives to control the density of the liquid medium. The latter contributes to environmental issues of waste media disposal (*3*).

Eddy current sorting is best suitable for sorting nonferrous metallic waste (*4*). The potential of this technology to achieve high recovery with lower energy consumption has revolutionized the nonferrous metallic scrap recycling procedure with much less environmental impact.

The eddy current separation method is based on the principle that the moving conducting material experiences a force in an alternating magnetic field (*5*). The induced

eddy currents in the nonferrous particles generate an opposing magnetic field which reacts to the external magnetic field, which in turn causes a particle to be repelled from the incident magnetic field. The deflection force is termed as the Lorentz Force. The magnitude of the force varies with the particle's electrical conductivity to density ratio and external field frequency, so at the optimal frequency various nonferrous metals and alloys can be sorted from one another.

Commercially available mechanical eddy-current sorters currently like the ones manufactured by Eriez Manufacturing (Erie, Pennsylvania) have a cylindrical drum with permanent magnets arranged on its circumference which produces frequency up to 1 KHz when rotated at high speed. At this low frequency the machine is capable of sorting particles of size greater than 1 in., but incapable of sorting particles smaller than 1 in.

The method discussed in this study is about using a variable AC frequency eddy current sorting (EDX) prototype to separate different nonferrous metal and alloys of size less than 1 in. in diameter. EDX is a solid state technology and can operate at a variable frequency range between 1 to 25 KHz. The AC magnetic field frequency plays an important role in sorting different nonferrous metals and alloys from one another other.

The nonferrous metals and alloy material mixture is fed into a gapped toroid. The toroid generates an AC magnetic field when alternating current passes through the winding on the toroid. On interaction with the external magnetic field, a particle develops eddy currents which produce an internal magnetic field that opposes the external magnetic field, resulting in deflection of the particle due to the Lorentz Force. This force deflects the particle away from the strong magnetic field region to the weak magnetic field region, resulting in particle separation (6). Optimal sorting occurs at the frequency

where the maximum difference in the deflection force is present, which results in one of the materials deflecting farther than the other. Ejection velocity calculation experiments confirm theoretical predicted optimal sorting frequency. The results for sorting various nonferrous metals and alloy mixtures will be discussed in detail in this thesis.

The EDX technology overcomes various limitations incurred by other eddy current sorting methodologies by eliminating the moving parts needed to produce the alternating magnetic field, thus resulting in less downtime and maintenance expense caused by wear and tear. Also in EDX technology operation, it is fast and easy to tune a wide range of frequencies. The potential of this sorting technology can lead to the manufacturing of industrial scale ruggedized units for commercial operations at various scrap sorting industries.

CHAPTER 2

LITERATURE SURVEY

Many eddy current sorting techniques have been developed to improve sorting efficiency of nonferrous metal recycling process. Since the 1960s various researchers have published their theories on eddy current separators while many of them have patented their technologies. In this chapter, various theories associated with eddy current sorting technologies will be described.

The eddy current sorting technique was known and developed over a hundred years ago and it is a widely studied and utilized phenomenon in designing electric dynamo, transformers, and motors. But the eddy current technique was overlooked as a method to sort a mixture of nonferrous materials into discrete similar nonferrous materials and also from nonconducting materials.

Schloemann (7) did a survey of eddy current separator techniques and his study is summarized in the following paragraphs.

Edison (8) introduced the conceptual technique to utilize the eddy current separation method to separate precious metal gold from a mixture of other nonferrous particles. During the same year Maxim (9) patented a technique to separate copper, gold, silver, and other nonferrous metallic materials from a mixture of other nonconductive materials. His magnetic separator technique involved rotating electromagnets powered by

DC currents to produce an alternating magnetic field effect. Moffatt (*10*) patented a technology in which stationary electromagnets were supplied with an alternating current to produce a high-frequency alternating magnetic field, the magnetic field repelled the nonferrous diamagnetic materials and attracted paramagnetic materials while insulating materials remained unaffected. The separation technique demonstrated the principle of repulsive force experienced by nonferrous metals in the presence of high-frequency alternating magnetic fields.

Isbell (*11*) patented a multiphase magnetic separator technology, which used an electromagnet to produce an alternating magnetic field to separate magnetic materials from less conductive nonferrous scrap material. Mordey (*12*) developed and patented a technology using a similar multiphase electromagnet to enrich mineral ores by separating magnetic mineral particles from nonmagnetic gangue materials.

McCarthy (*13*) patented a metal concentration technology, which could separate metals with similar electrical conductivity but differing magnetic coefficients by utilizing an alternating magnetic field produced by alternating current electromagnets. Benson and Falconer (*14*) designed an electrodynamic separator that could separate materials with a large difference in conductivity by using an electromagnet to excite eddy currents into the materials. British Thompson-Houston Company (*15*) and Lee (*16*) utilized principles of high-frequency eddy current separation in their technologies. Lovell (*17*) displayed a separation technology that utilized coils excited by high frequency currents. Suitably arranged coils can neutralize repulsive force and can keep nonferrous particle stable at the same position and other nonmagnetic particles are pulled down by the gravity. Benowitz (*18*) patented a technique which used high-frequency excited coils setup to separate

conductive materials from nonconductive and nonmagnetic materials.

Major advancement in eddy current separator technology was contributed by researchers at Vanderbilt University (*19*) during the 1960s. A separator using a linear motor type electromagnet was developed and extensively tested. The linear motor was powered by 60 Hz alternating current covered by a conveyer belt to move material over an alternating magnetic field. Another unique approach developed at Vanderbilt University was the technique in which free falling particles were allowed to pass through the path of unbalanced magnetic field gradients (*20*), and separators using a rotating assembly of DC electromagnets and permanent magnets (*21*).

Zalcharova (*22*) patented a technique using two electromagnets arranged in the manner in which the magnetic fields lines are perpendicular to each other. The top electromagnet's field deflects the asymmetrically falling particle to the orientation which results in the particles exposure to the second electromagnet with a maximum cross sectional area resulting in the maximum deflection force experienced by the nonferrous materials. This technique lacked appropriate theoretical background and was never practically proved.

Morey et al (*23*) used the linear motor technique to separate larger sized nonmagnetic and electrically conductive materials. The linear motor was powered with alternating current at frequencies ranging from 400 to 800 Hz. Due to low frequency the technology was not capable of sorting particles smaller than 6 mm size. Laithwaite (*24*) used a similar technique of linear motor to separate nonferrous scrap material.

Reid (*25*) developed a technique to sort nonmagnetic particles by controlling the magnetic flux generated by the electromagnet. Eddy current was produced on the surface

of the nonmagnetic particles which exerted a unidirectional force on the particle resulting in the separation of nonmagnetic material from other nonmetallic materials.

Complexity of construction associated with eddy current separators based on electromagnets made them less popular compared with eddy current separator based on permanent magnets. With advancements in developing stronger permanent magnets, high efficiency separator was developed for nonferrous material sorting applications from automobile scrap and shredded solid municipal waste (*26-29*). Because of unable to produce high-frequency an alternating magnetic field, mechanical eddy current sorters are unable to separate particle size less below 5 mm (*30*).

To develop new theoretical eddy current sorter design, it was important to study and understand the interaction of nonferrous conducting particles with alternating magnetic fields. Schloemann (*31*), Braam et al. (*32*), Schubert (*33*), Van der Valk et al. (*34*) contributed in developing the theoretical models by performing and studying experimental research on vertical eddy current separators (VECS), rotating disk separators, and ramp eddy current separators (RECS). Theoretical models were verified on VECS and different prototypes of RECS.

Lohofer (*35*) used electromagnetic coils set up to levitate nonferromagnetic conducting spheres. He derived an analytical equation to calculate power absorbed and the force experienced on spheres due to eddy current induction by an external alternating magnetic field. Woltereck et al. (*36*) explained the use of levitation-based eddy currents for sorting aluminum pieces from waste streams. Experimental, numerical, and analytical techniques were used to investigate eddy currents induced and force experienced by the particles. Finite element analysis technique was also used to analyze the force acting on an

aluminum particle placed over multiple electromagnets coils arrangement. The finite element model was verified by comparing two methods: the moving image method for thin plates and Laplace transformation techniques for a conducting half space.

Rem et al. (*37*) at Delft University of Technology developed a mathematical model for eddy current separation technique. The model focuses on predicting the motion of particles during eddy current separation. The model showed qualitative confirmation with experimental data on the effect of particle conductivity, shape, and size. The model also predicted particle motion for simple shaped particles using numerical integration. Rem et al. (*38*) also presented an improved simulation model for rotary drum-based eddy current separators. The model improvised a first-order differential equation of the magnetic moment of nonferrous materials in an alternating magnetic field. The model also explained the mechanical interaction between a conveyor belt and the nonferrous particles during transportation and aerodynamic forces interacting during the separation process. The new model was able to better predict the particle deflection with a relative error of 10% at normal operating conditions. The accuracy of the model was not greatly affected by the friction force imparted on nonferrous particles during their contact with the belt but large changes in simulated results were observed when input parameters were slightly changed.

Fraunholez et al. (*39*) found that high deflection force is produced on copper cylinders placed inside transparent vessels filled with water when exposed to alternating magnetic fields. The experiment was done using granular and flat metal particles ranging from 1 to 3 mm in length and a varying magnetic field was produced by permanent magnet rotor used in a standard eddy current separator. The particles showed a horizontal deflection of 10-30 cm away from the magnetic field source.

Lungu and Rem (*40*) developed a eddy current sorter setup called single disk eddy current separator (SDECS). They used a slanted horizontal rotary disk fitted with permanent magnets aligned alternatingly in south-north and north-south orientation. The disk was connected by a shaft to an electric motor. The SDECS was developed to separate nonferrous particles size smaller than 5 mm from other nonmetallic particles found in electronic wastes.

Lugnu, (*41*) used a dynamic eddy current separator device called angular drum eddy current separator (ADECS). He showed that ADECS can be used to separate smaller size nonferrous particles mixed with other nonferrous materials. The device consisted of a horizontal drum on which permanent magnets were placed. The magnets were arranged with an alternating orientation of S-N and N-S polarity. A conveyor belt was placed over the magnetic roller covering the whole drum. The drum when rotated, creates an alternating magnetic field and nonferrous particles when exposed to the magnetic field start jumping, resulting in separation. When the drum was inclined to 45°, maximum separation efficiency was achieved. The efficiency of ADECS was similar to other dynamic eddy current separators but simple construction of ADECS made it cheaper to operate compared to other nonferrous sorting techniques.

Saveliev (*42*) patented a technique in which a toroidal-shaped ferromagnetic core with a pie-shaped gap was cut into it. The core was made by sintering technique using ferrite powder. The core was wound with wire then an alternating current was supplied to it. The wound core acted as an inductor and induced an alternating magnetic field in the cut. When nonferrous materials are fed into the gap cut, eddy currents are induced into the materials and are deflected away from the core. This technique was able to produce high

frequency magnetic fields up to 25 kHz which makes separation of smaller size nonferrous particles easier. The experimental technique presented in this follows Saviliev's ferrite core and excitation frequencies

CHAPTER 3

THEORIES: EDDY CURRENT SEPARATION

Many theories have been derived to develop different types of eddy current separation techniques. A brief explanation of different fundamental theories is mentioned in this chapter. Finally, the theory on which this experimental study is based on, is discussed.

3.1 Fundamental: eddy current separation

When a charged particle travels through an electromagnetic field, it experiences a force which is combination of an electric force $\vec{F}_e$ and a magnetic force $\vec{F}_m$. This combined force is known as the Lorentz force (*44*) and is given by

$$\vec{F} = \vec{F}_e + \vec{F}_m, \tag{3.1}$$

where the forces $\vec{F}_e$ and $\vec{F}_m$ are then given by

$$\vec{F} = q\vec{E} + q\vec{v} \times \vec{B}, \tag{3.2}$$

where q is the charge, $\vec{v}$ is the velocity, $\vec{E}$ is the electric field and $\vec{B}$ is the magnetic field.

For the condition where the conducting particle experiences only a magnetic field, the force component due to the electric field from Equation 3.2 can be neglected, which leaves only magnetic force,

$$\vec{F}_m = q\vec{v} \times \vec{B} \tag{3.3}$$

For a continuous flow of electrical current density $\vec{J}$, we would use the more general expression of the differential force $d\vec{F}$ acting on a differential volume dV in a rigid body, which is written as,

$$d\vec{F} = \left(\vec{J} \times \vec{B}\right)dV \tag{3.4}$$

When all the individual differential forces acting on a differential volume of the rigid body are integrated, we get total force acting on the rigid body, which is expressed as,

$$\vec{F} = \int d\vec{F} = \iiint (\vec{J} \times \vec{B})dV \tag{3.5}$$

Next, according to Faraday's law, a changing magnetic field induces electric field in accordance with

$$\nabla \times \vec{E} = -\frac{\partial \vec{B}}{\partial t} \tag{3.6}$$

Now, applying the point form of Ohm's law, which states that conducting particle in presence of electric field $\vec{E}$ produces electric current density $\vec{J}$,

$$\vec{J} = \sigma\vec{E} , \qquad (3.7)$$

where σ is the electrical conductivity of the particle. However, as shown in Equation 3.5, current density is related to magnetic force acting on the particle. Thus, electric fields are created by changing magnetic field, which in turn creates electrical currents. This explains the relation of magnetic force exerted on the particle when it is in presence of an external alternating magnetic field. Electrical currents are produced in the particle when it is exposed to an alternating magnetic field. The path of the currents resembles small whirlpools formed in a flowing river stream so they are called eddy currents.

When the conducting particle is exposed to external magnetic fields, it also experiences a torque $\vec{\tau}$. So from the definition of torque around the center of mass of the particle, we know that,

$$\vec{\tau} = \vec{r} \times d\vec{F} \qquad (3.8)$$

where $\vec{r}$ is the distance between the point of force application and the particle's center of mass. Substituting Equation 3.4 in Equation 3.8 gives torque in terms of current density

$$\vec{\tau} = \iiint \vec{r} \times (\vec{J} \times \vec{B}) dV \qquad (3.10)$$

For special cases when B field is constant, torque $\vec{\tau}$ is expressed as,

$$\vec{\tau} = \left(\iiint \vec{r} \times \vec{J} dV \right) \times \vec{B} \tag{3.11}$$

Let $m = \iiint \vec{r} \times \vec{J} dv$ where $\vec{m}$ is the magnetic moment, so Equation 3.11 can be written as

$$\vec{\tau} = \vec{m} \times \vec{B} \tag{3.11}$$

It can be shown that for constant $\vec{B}$, $\vec{F}$ is zero (*45*). However, when spatially varying particles are present in an external magnetic field with gradient, it is possible to show that

$$\vec{F} = \nabla \left(\vec{m}.\vec{B} \right) \tag{3.12}$$

In eddy current sorting, particles are subjected to magnetic field with varying gradients which causes them to deflect away. However, deflection force varies based on the magnetic field gradient available in the sorting system.

3.2 Mechanical eddy current separator model

Rem et al. (*37*) along with other researchers at the Delft University of Technology developed a model to calculate trajectory motion of the particles sorting in an eddy current separator.

The model considers various forces acting on particles like gravity, frictional forces due to a conveyor belt, air and electromotive forces to determine deflection trajectory. As

nonferrous particles deflect away from the alternating magnetic field, particles sense variable magnetic flux due to simultaneous rotational and translational motion. So considering *U(t)* to be the transformational axis coordinate between the lab frame and particle frame, *B(r,t)* to be the magnetic field and *B(t)* to be the vector of magnetic field. Then,

$$U(t).B(t) = \text{B}(r(t), t) \tag{3.13}$$

Then with respect to time variation of *B* and *U* is given by

$$U.\frac{d}{dt}B(t) = \frac{\partial B}{\partial t} + (u \cdot \nabla)B - \Omega \times B \tag{3.14}$$

$$\frac{dU}{dt} = \Omega \times U \tag{3.15}$$

Where, *U* and *Ω* are its translational and rotational velocities, respectively, and *r(t)* is the position of the particle.

So, the Lorentz force for a small particle is given by

$$\vec{F} = M \cdot \nabla B \tag{3.16}$$

and torque is given by,

$$\tau = M \times B \tag{3.17}$$

Where, *M* represents the magnetic moment of the particle.

3.3 Horizontal rotating disk and vertical eddy current separators

Researchers at Delft University of Technology, Netherlands, did broad research in developing horizontal disk and vertical eddy current separators and also developed a model to simulate a force acting on nonferrous materials during separation process. Their research indicated that magnetic induction acting on a particle is similar in both types of eddy current separators setups. Also, their model calculated repulsive forces acting on a solid block-shaped particle are similar in both types of eddy current sorter setups.

Van der Valk et al. (*46*) presented the boundary condition and the solution for the differential equation and the derived resultant repulsive forces are given as follows

$$F_x = -m\alpha_{xx}v_x + m\alpha_{xz}v_z \tag{3.18}$$

$$F_x = 0 \tag{3.19}$$

$$F_z = m\alpha_{xz}v_x - m\alpha_{zz}v_z \tag{3.20}$$

Where '*m*' is the mass of the particle; v_x and v_z are the velocity components along *x* and *z* axes, respectively; α_{xx}, α_{xz}, and α_{zz} are damping coefficients.

In the case of vertical eddy current separators, the particle moves parallel to the

vertical XY plane, so α_{xz}, changes with time. The periodic average forces acting in the x direction is given by

$$F_x = -m\beta v_x \tag{3.21}$$

where 'β' is the time average of the damping coefficient 'α_{xx}' and is considered to remain constant during the process when a particle passes through the vertical passage channel in a vertical eddy current separator. So β is given by

$$\beta = \frac{1}{4}\frac{\sigma}{\rho}a^2 D\left(\frac{a}{b}\right)\sum_{n=1}^{\infty}\left(\frac{2\pi n}{\lambda}B_n\right)^2 + T(z) \tag{3.22}$$

where ρ is the specific density of a particle; σ is the electrical conductivity of the particle; a, b, and c are the dimensions of the block particle in x, y, and z axes; n is the an integer, and λ is the period of the strip magnetization. $T(z)$ is the function depending on the z coordinate. $T(z)$ is given by

$$T(z) = \frac{1}{4}\frac{\sigma}{\rho}\left\{a^2 D\left(\frac{a}{b}\right) + c^2 D\left(\frac{c}{b}\right)\right\}\sum_{n=1}^{\infty}\left\{\frac{2\pi n}{\lambda}B_n \sinh\left(\frac{2\pi n z}{\lambda}\right)\right\}^2 \tag{3.23}$$

where D is the function of $p = a/b$ or c/b and it is given by

$$D(p) = \left(\frac{2}{\pi}\right)^4 \sum_{n=1}^{\infty} \sin^2\left(\frac{\pi n}{2}\right)\frac{1}{n^4}\left\{1 - \frac{2p}{\pi n}\tanh\left(\frac{\pi n}{2p}\right)\right\} \tag{3.24}$$

In the case of a rotating disc eddy current separator, due to the rotational motion of the disk and the motion of the particle itself, a change in magnetic induction due to induced eddy current the force is exerted on the particle which is given by,

$$Ft = m\beta.(R)(2\pi vR - v_t) \tag{3.25}$$

Where, v is the frequency of the rotating disk, m is the mass of the particle, R is the radius of the rotating disk and v_t is the tangential component of the velocity of the particle.

3.4 Modified Saviliev's eddy current separator model

Saviliev [42] gave a theoretical model for a solid state eddy current separator using a magnetic field produced by a ferrite torroid. Kip (*47*) in his thesis research work, examined the model and came up with the theoretical explanation about the forces acting on the electrically conducting particle. Naidu (*48*) and Saurabh (*49, 50*) used this model to conduct experiments to separate fine size nonferrous materials from various industrial waste streams. The theory is explained as follows:

An alternating magnetic field can be written as

$$\vec{B} = \vec{B}_0 e^{i\omega t} \tag{3.26}$$

For spheres, magnetic moment $\vec{M}$ is related to $\vec{B}$ field by

$$\vec{M} = \alpha V_p \vec{B} \tag{3.27}$$

where Vp is the volume of the particle and α is the coefficient of magnetic polarization which is a function of real and imaginary magnetic polarization which further are the function of frequency f, electrical conductivity σ, and the particles diameter d. The coefficient of magnetic polarization is given by,

$$\alpha = \alpha' + \alpha''i \tag{3.28}$$

where,

$$\alpha' = \frac{3}{8\pi}\left[1 - \frac{3\delta r \sinh\left(\frac{d}{\delta}\right) - \sin\left(\frac{d}{\delta}\right)}{2r \cosh\left(\frac{d}{\delta}\right) - \cos\left(\frac{d}{\delta}\right)}\right] \tag{3.29}$$

and

$$\alpha'' = \frac{9\delta^2}{16\pi r^2}\left[1 - \frac{r \sinh\left(\frac{d}{\delta}\right) - \sin\left(\frac{d}{\delta}\right)}{\delta \cosh\left(\frac{d}{\delta}\right) - \cos\left(\frac{d}{\delta}\right)}\right] \tag{3.30}$$

where δ is the skin depth and is given by

$$\delta = \sqrt{\frac{2}{\mu_o \omega \sigma}} \tag{3.31}.$$

Deriving the unit of skin depth using the SI unit values of, $\mu_0 = 4\pi \times 10^7$ m kg s^{-2} A^{-2}, $\omega =$

$2\pi f\, s^{-1}$ and $\sigma = m^{-3}\, Kg^{-1}\, s^3\, A^2$, skin depth '$\delta$' is inversely proportional to the square root of frequency which indicates that at higher frequency, the skin depth is smaller and vice versa.

The force experienced by an electrically conductive particle in the presence of a magnetic field is expressed as

$$\vec{F_B} = (\nabla \cdot \vec{M})\vec{B} \tag{3.32}$$

It is known that that the magnetic moment $\vec{M}$ leads the magnetic field vector $\vec{B}$ by an angle θ and is given by

$$\theta = \tan^{-1}\left(\frac{\alpha''}{\alpha'}\right) \tag{3.33}$$

At lower frequencies, magnetic moment phase $\vec{M}$ leads the magnetic field vector $\vec{B}$ by 90^0 and in that case the average force is zero. At higher frequency, the magnetic moment phase $\vec{M}$ is the same with respect to that of magnetic field vector $\vec{B}$ and the average force at that situation is given by

$$<\vec{F_B}> = \frac{1}{4}\alpha' V_p \nabla \left|\vec{B_o}^2\right| \tag{3.34}$$

At medium frequencies, phase angle between magnetic moment $\vec{M}$ and magnetic field vector $\vec{B}$ differs from 0^0 to 90^0. The generalized force, in this situation is given by

$$< \overrightarrow{F_B} > = \frac{1}{4}\gamma C V_p \nabla |\vec{B}_0|^2 \tag{3.35}$$

where γ is cosθ and C is given by $\sqrt{\alpha'^2 + \alpha''^2}$.

The gravitational force acting on the particle is given by

$$m\vec{g} = -\nabla u \tag{3.36}$$

Superimposing the magnetic force and gravitational force acting on the particle gives the final dynamic force acting on the particle and it is given by

$$\vec{F} = \frac{\gamma C V_p}{4} \nabla |\vec{B}_0|^2 - \nabla u \tag{3.37}$$

Hence, the total energy particle contain while passing through the electromagnetic field is given by

$$E = \frac{mv^2}{2} + mgz - \frac{\gamma C V_p}{4} \nabla |\vec{B}_0|^2 \tag{3.38}$$

The ejection velocity of the particle passing through the air gap is given by

$$v = \sqrt{\frac{\gamma C}{2\rho}} |\vec{B}_0| \tag{3.39}$$

where γ is the multiplication factor, C is $\sqrt{\alpha'^2 + \alpha''^2}$, ρ is particle density, and B_0 is the

magnetic field strength at the initial position from where the particle starts experiencing the magnetic field.

Most of the theoretical foundation and the mathematical basis used by Saveliev in his patent has been referenced from the physical model of Landau and Lifshitz (*51*). However, mathematical calculations used to develop the physical model contains many assumptions which makes the model limited in its scope and applicability. On comparing Equations 3.27 and 3.32, both the equations contain magnetic moment but their S.I units do not match up while deriving the units individually, which supports the fact that Saveliev's model has limited scope. In developing further analytical models, this line of reasoning was abandoned as a result.

3.5 Lohofer levitation theory model

The physics behind the eddy current separation used in this thesis is based on Lohofer's (*35*) work on analytical solution of power absorbed and force experienced by conducting metallic sphere exposed to an alternating magnetic field. The equation developed by Lohofer is explained and extended as necessary.

A conducting particle exposed to alternating magnetic field experiences Lorentz force which is given by

$$F = -\nabla(m.B) \tag{3.40}$$

Where m is the dipole moment and B is the magnetic field intensity. Expanding the equation 3.40 by inserting expression for magnetic dipole moment of a conducting non-

ferromagnetic material sphere, then the time averaged force experienced by the sphere was

given by [50]

$$F = -\frac{\pi R^3}{\mu_0} G(q) \, grad B^2 \tag{3.41}$$

where *G(q)* is a function given by

$$G(q) = 1 - \frac{3}{2q} \frac{sinh(2q) - sin(2q)}{cosh(2q) - cos(2q)} \tag{3.42}$$

Where $q = R/\delta$, where *R* is radius and is δ skin depth given by $\delta = \sqrt{2/\omega\sigma\mu_0}$, where σ is

the conductivity of the material.

Considering a single direction of $\vec{B}$ and one component of it in one direction only, Equation

3.41 can be also written as

$$F = -\frac{\pi R^3}{\mu_0} G(q) \frac{\partial}{\partial x} \left(B^2(x) \right) \tag{3.43}$$

Physical work exerted on the particle as it deflects away from the gap may be calculated as

$$W = \int_{B_0}^{0} F dx \tag{3.44}$$

The lower limit will be B_0, which is the initial magnetic field experienced by the particle at the narrow end of the gap and the upper limit will be 0 as particle exits the gap where magnetic field intensity drops to zero. This assumes that there is no phase change in the magnetic field once the particle exits the gap. So, substituting for F from Equation 3.43 to Equation 3.44

$$W = \int_{B_0}^{0} -\frac{\pi R^3}{\mu_0} G(q) \frac{\partial}{\partial x}\left(B^2(x)\right)\partial x \tag{3.45}$$

$$W = \int_{B_0}^{0} -\frac{\pi R^3}{\mu_0} G(q) \frac{\partial}{\partial x}\left(B^2(x)\right)\partial x \tag{3.45}$$

$$W = -\frac{\pi R^3}{\mu_0} G(q) 2B \int_{B_0}^{0} B\partial x \tag{3.46}$$

$$W = -\frac{\pi R^3 B}{\mu_0} G(q) B]_{B_0}^{0} \tag{3.47}$$

$$W = \frac{\pi R^3 B_0^2}{\mu_0} G(q) \tag{3.48}$$

As there is no significant amount of friction acting on the particle when it is deflected away from the gap, we can assume that all of the energy is converted into kinetic energy. Hence Equation 3.47 can be equated with kinetic energy, that is, $1/2mv^2$ and from that we can find the exit velocity of the particle which is given by:

$$v = \sqrt{\frac{2W}{m}} \tag{3.49}$$

where, m is the mass of the particle and W is the work done derived in equation 3.48

CHAPTER 4

EXPERIMENTAL SETUP

An experimental setup unit model of electrodynamic sorter (EDX) was constructed using various components which were electrically connected with each other to form a resistor-inductor-capacitor (RLC) circuit. The experimental system consisted of a gapped ferrite core wound with electrical wire to form an inductor, capacitors, a power amplifier with internal DC power source, a function generator, a 1 Ω power resistor, an oscilloscope, a vibratory feeder, and a catchment or collector box with splitter. A schematic diagram of EDX is shown in Figure 4.1
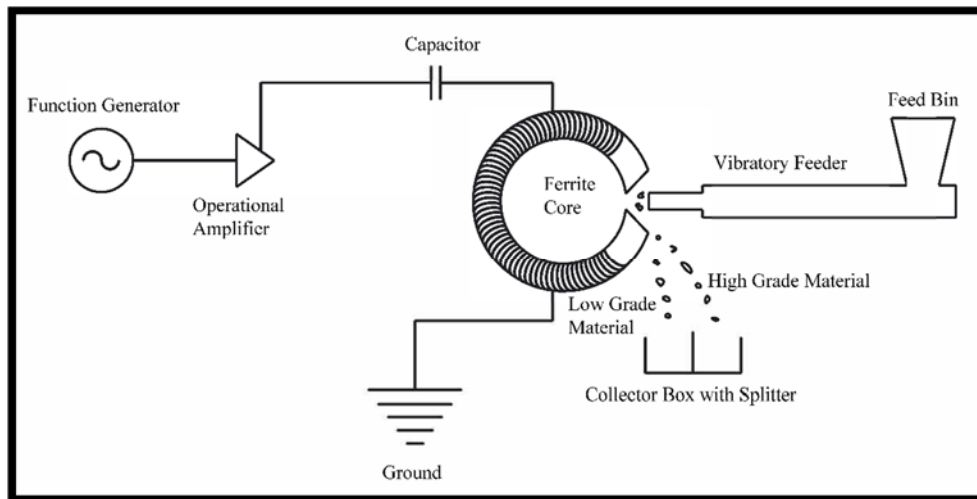
Figure 4.1. Schematic diagram of the experimental setup

4.1 Components of EDX experimental unit

Components used to assemble an experimental EDX setup are shown in Figure 4.2. The components used are listed in Table 4.1 and are also briefly described follow.

4.1.1 Magnetic core

A ferrite core was used to make an electromagnet for EDX experiments. Electrical wire is wound around the toroid to create an electromagnet. The number of turns to be wound depends on the required inductance required for the circuit. Electrical wire must have sufficient insulation to sustain high voltages produced at resonance. All cores used in

Figure 4.2 EDX experimental setup (Photograph © Nakul Dholu 2016)

Table 4.1 List of equipment used

Component	Model Number	Manufacturer
Operational Amplifier	7796-0215-0187	AE Techron
Oscilloscope	TBS 1064	Tekronix
Function Generator	33210A	Keysight
Vibratory feeder	HS26	Eriez Magnetics
Capacitors	273 Series	Cornell Dubilier

this experiment were wound with wire having a breakdown voltage of above 12 kV. Core

specification are given in Table 4.2

4.1.1.1 Ferrite core

Ferrite core was used as key component of EDX. When excited, an alternating

magnetic field was produced at the air gap and nonferrous material were fed into the gap

for sorting. Two different types of ferrite cores were used to perform sorting experiments.

A sandwich core made of two ferrite cores manufactured by Magnetics® (0W49740TC)

were used to sort a mixture of Al, Cu, Brass, and Titanium 6-4 spheres of 6 mm diameter

in size. The sandwich core had an inner gap of 2mm and 35 mm for the outer gap. A NiZn

Ferrite core manufactured by National Magnetics Inc. was used for ejection velocity and

Zorba sorting experiments. The core had a complex cut with an effective feed gap

dimension of 10mm and outer gap of 20mm. Figure 4.3 and 4.4 shows a 3D view of both

cores with dimensions. The core is manufactured using powder metallurgical technique.

All the grains of the ferrite materials are oriented to the same optimal direction so that the

core has good magnetic flux permeability when excited. Proper care was required while

machining the core to obtain complex cut geometry gap. Ferrite cores have the ability to

perform well at frequency range of 1 KHz to 30 KHz so they are well-suited for eddy

Table 4.2 List of cores used in EDX experiments

Core	Material	Inner Gap (mm)	Outer Gap (mm)	Height (mm)	ID (mm)	OD (mm)
0W49740TC	Ferrite	2	30	25	106	140
CMD	Ferrite	10	20	30	240	440
CRGO	Steel	5	40	78	175	250
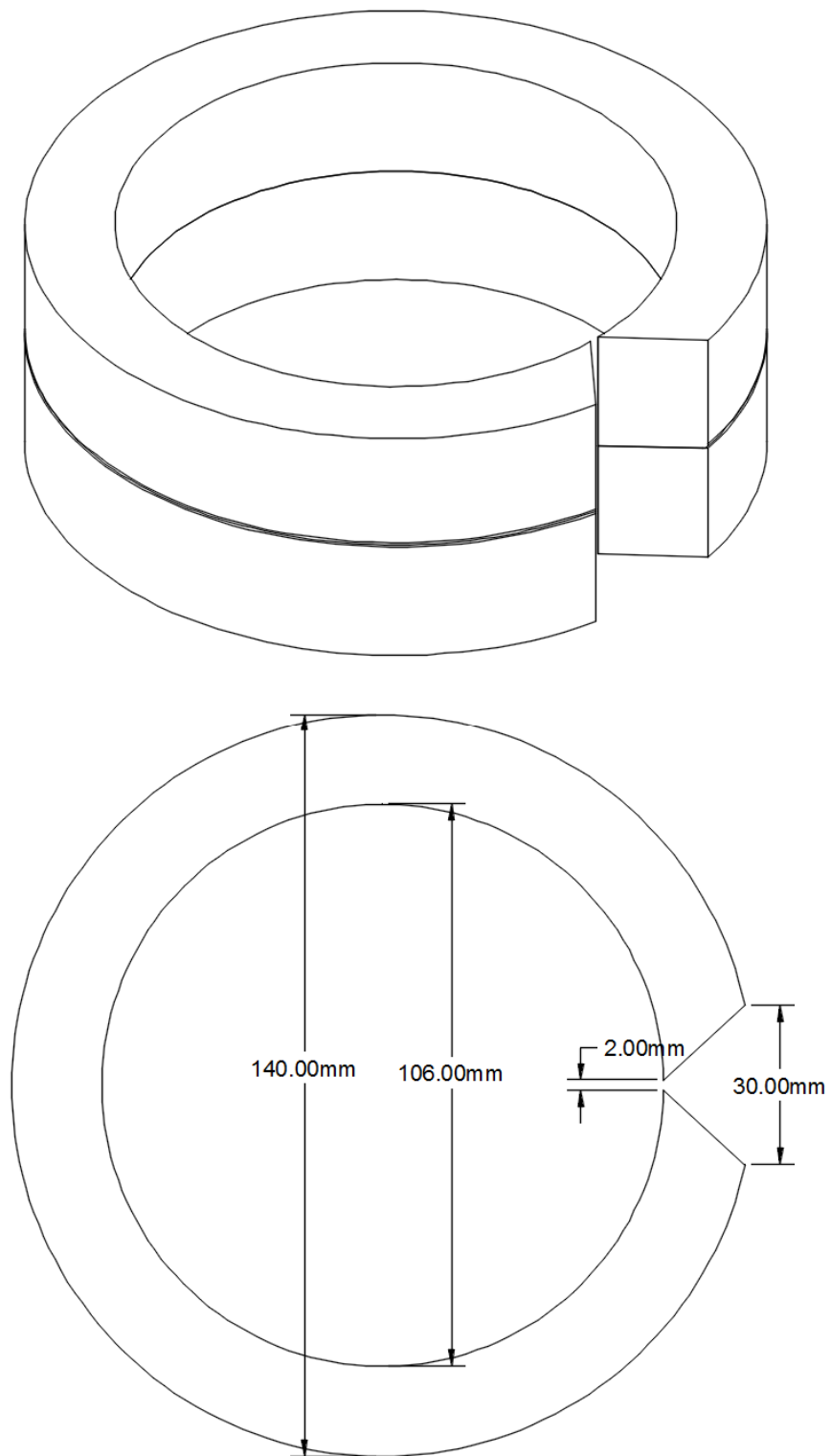
Figure 4.3 3-D design view of a stacked ferrite core used in metal/nonmetal sorting experiments
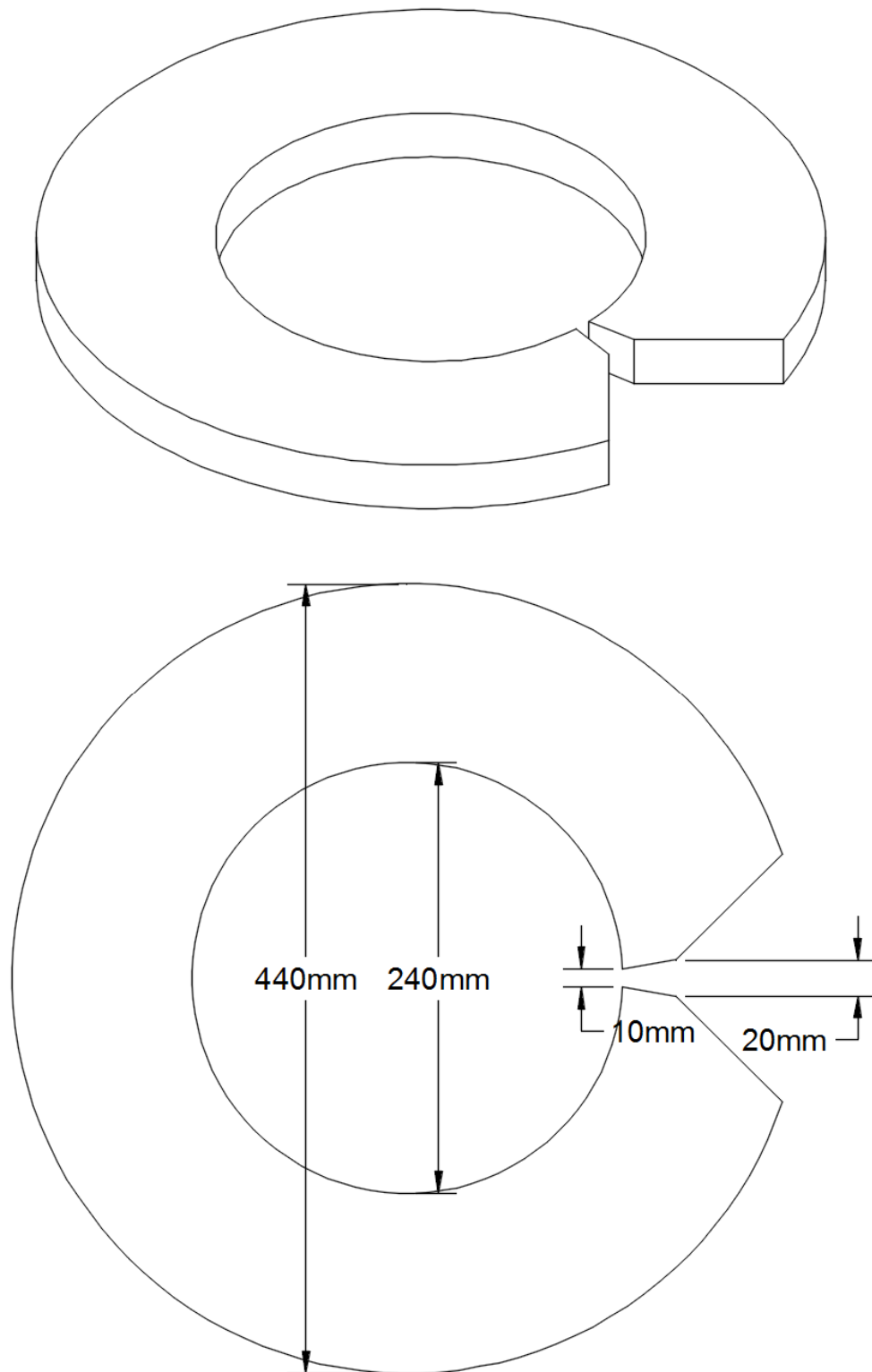
Figure 4.4 3-D design view of CMD core used in velocity experiments and scrap sorting experiments

current sorting with wider range of frequency operation.

4.1.1.2 Cold rolled grain oriented core

Cold Rolled Grain Oriented (CRGO) silicon steel core was used to perform aluminum alloy coupon sorting experiments at lower frequencies below 1 kHz. CRGO core is made from laminated silicon steel which has a very high magnetic field saturation (i.e., above 1 T at low frequencies). Hence it is best suited for Al alloy sorting by eddy current. The core used had inner gap cut of 5 mm and outer gap cut of 40 mm. In order to achieve consistent feeding of aluminum coupons into the gap, an add-on fixture made of a Delrin was inserted into the gap of the core. The fixture had a chamber to feed aluminum coupons from the top and was designed for the purpose to keep coupons into a fixed orientation where the maximum cross section is available to induce eddy currents into it. Delrin is permeable to the magnetic field and can also withstand temperatures range around 200°C without physically deforming, hence, it was best suited for this application. Figures 4.5 and 4.6 show a 3D view of CRGO core and core with Delrin fixture.

4.1.2 Operational amplifier

The AE Techron (7796) amplifier with integrated DC power supply was used to amplify signal input provided to by the function generator to the circuit. The amplifier contains transistors connected in specific circuit arrangement to amplify the input signal using the DC power source from the integrated DC power supply. The amplifier has 20 times signal amplification capability with power range of 4000 W. The amplifier also had a protection circuit which disconnects the amplifier circuit in case of over temperature,
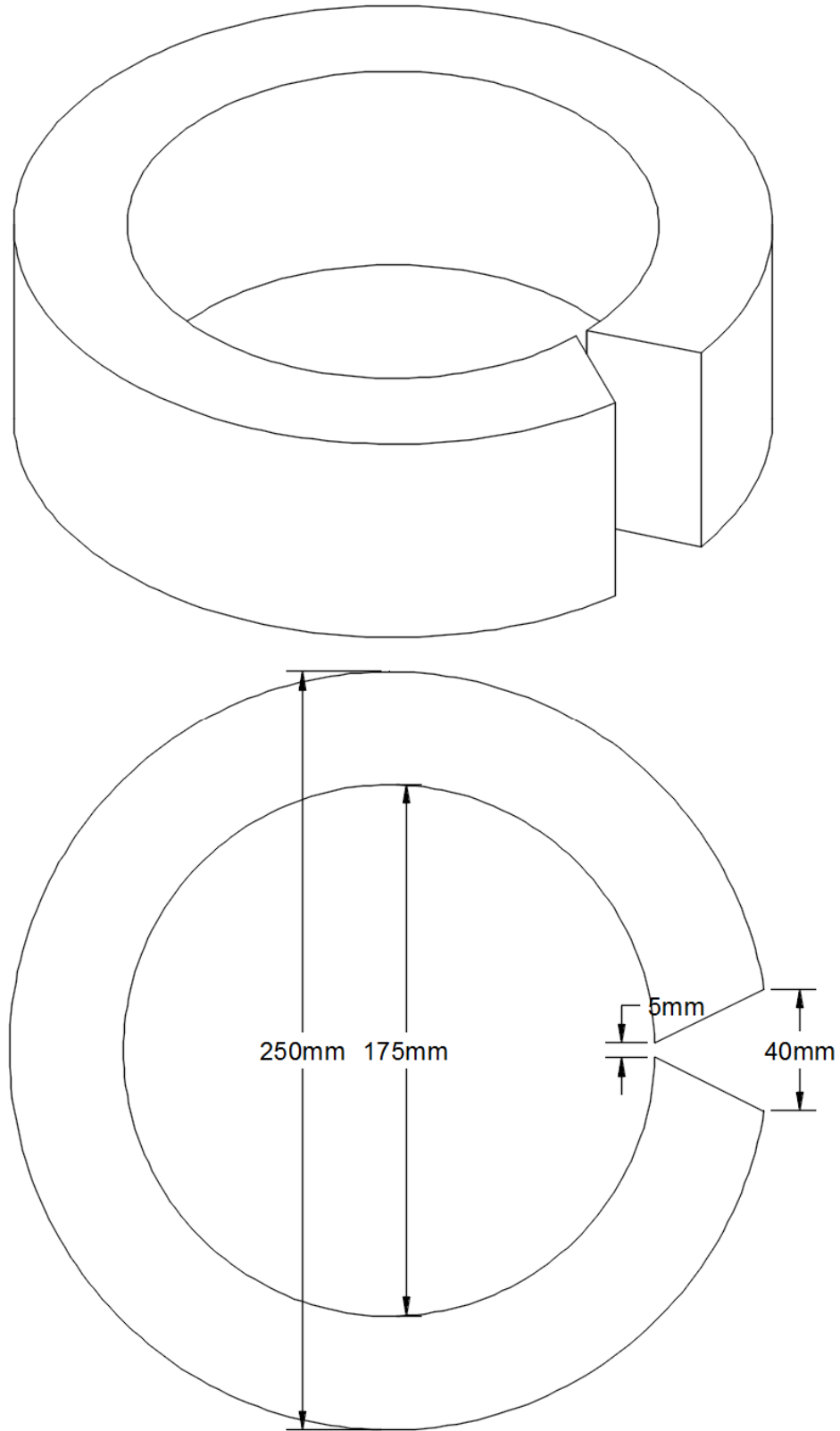
Figure 4.5 3-D design view of a CRGO core used in Al alloy coupon sorting experiments

Figure 4.6 CRGO core with Delrin fixture (Photograph © Nakul Dholu 2016)

shorted improper load, over current, and high supply voltage. Overall it provides fast slew rates and very low noise and is optimized to drive low impedance loads.

4.1.3 Function generator

A 10 MHz Keysight (33210A) digital function generator was used to set resonance frequency input to the amplifier. Signal voltage can also be set using this function generator. The knob was used to change frequency linearly and a numeric keypad was used to provide exact frequency input to the circuit.

4.1.4 Oscilloscope

A multichannel 150 MHz Tektronix (TBS 1064) digital oscilloscope was used in the EDX experimental setup. Two different channels were used to measure current flowing through the coil and also to measure AC voltage across the core. AC voltage was measured using 1000X attenuating probe.

4.1.5 Capacitor bank

Mica capacitors with high break down voltage and high current handling with capacitance ranging from 5 nF to 20 nF were used in the experimental setup. Discrete numbers of capacitors were used to form a capacitor bank. To change out the operating frequency of the experimental setup, capacitors can be added or removed from the bank. The capacitor bank setup provided safe and better space management. Figure 4.7 shows the capacitor bank used for the experiment.

Figure 4.7 Capacitor bank with discrete capacitors (Photograph © Nakul Dholu 2016)

4.1.6 Vibratory feeder

A vibratory feeder manufactured by Eriez Magnetics (HS26) was used to feed material into the ferrite core's air gap. The material was transferred from a feed bin into the vibratory feeder which then transfers the material to the core gap. An add-on plastic tray was attached on the vibratory feeder to separate the metallic tray of the vibratory feeder from the air gap of the magnet in order to avoid magnetic coupling. Optimizing the feed speed was required to avoid material pile up at the air gap and was achieved by adjusting the vibration amplitude of the feeder. Also, an optimal feed height was required to feed material in order to avoid the effects of repulsive forces acting on the particles and to provide precision feeding to the air gap, thus, the feeder height was also adjusted accordingly. Figure 4.8 shows the vibratory feeder with plastic extension.
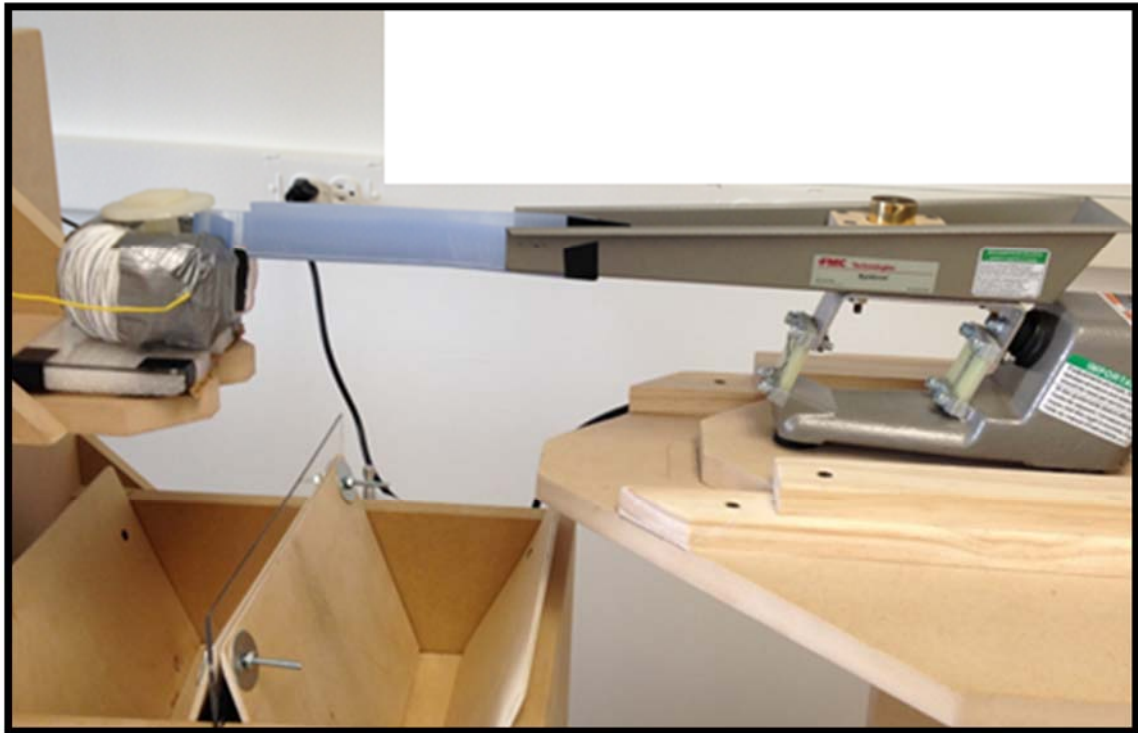
Figure 4.8 Vibratory feeder with plastic extension (Photograph © Nakul Dholu 2016)

4.2 EDX experimental unit setup and startup

All the components required for the EDX experimental setup were properly connected to form an RLC circuit. Operational amplifier, function generator, oscilloscope, and vibratory feeder were connected to a regular 120 V AC power source. The electromagnet core, capacitor bank, 1 ohm resistor and amplifier were connected in series with one another. A function generator was connected to amplifier to provide frequency input. A 1000X attenuating probe was connected to the oscilloscope in parallel with the coil to measure coil voltage. Another probe connected with oscilloscope was connected across the 1 ohm resistor to measure current in the inductor. To avoid electrical shocks and electrical hazards, all the equipment were kept switched off until the whole circuit was completely connected.

4.2.1 Operation of EDX circuit

Once the circuit was completely set up, the following steps were followed to excite the coil to resonance to perform eddy current separation experiments.

1. Power amplifier, oscilloscope, and function generator connected to power source are switched on.

2. The input voltage from the function generator was increased to 1V.

3. The resonance frequency was selected on the function generator. The resonance frequency is calculated using the formula as shown:

$$f = \frac{1}{2\pi\sqrt{LC}}$$

Where *L* is the inductance of the coil and *C* is the capacitance. The inductance of the coil was calculated using an LCR meter.

4. The output switch on the function generator is turned on to provide input to the amplifier. High-frequency vibration sound was heard, which indicated that the circuit is on resonance.

5. Voltage and current were monitored on the oscilloscope. Also, sine wave form of the voltage and current was observed using the oscilloscope.

6. The input voltage were increased from 1V just below where the voltage waveform clipped. Also, frequency was fine adjusted to achieve the exact resonance frequency based on current measurements.

7. Then the vibratory feeder was turned on and the material was allowed to fall through the air gap of the core.

8. The collector box with splitter was moved accordingly to collect the sorted material efficiently.

4.3 Pendulum experiment setup

An experiment to calculate the ejection velocity of different nonferrous material was performed to compare the theoretical model used to predict force acting on the particles during eddy current sorting at given frequency and also to study the effect of particle size and frequency on the deflection force of the particle. The experiment was performed using aluminum, copper, brass, and titanium spheres with diameters of 12 mm, 8 mm, 6 mm, and 4 mm at different frequencies ranging from 1 kHz to 8 kHz. To keep the material property like chemical composition and conductivity of each material constant, all the spheres of an

individual material type were machined from a cylindrical rod to get different sizes of spheres. Spheres were tied with thread and allowed to hang like a pendulum. A hanging sphere was placed inside the air gap of the core. A high speed camera manufactured by Fastec Imaging (InLine Camera) capable of capturing high speed videos at 1000 frames per seconds (fps) was used to capture deflection of a sphere. The high speed camera was placed vertically on the tripod stand so that the sphere's deflection could be captured from the bottom, looking upward. Deflection videos for the experiment were captured at 250 fps. Video digitizing software (MaxTRAQ) was used to analyze high speed deflection videos by frame by frame. Finally, mathematical data generated by digitizing video were used to calculate ejection velocity of the spheres, which is discussed in next chapter of this thesis. The pendulum experiment setup is shown in Figure 4.9

4.4 Factors associated with EDX performance

Variable-frequency eddy current sorting technique has various associated variable factors which effect the sorting performance. Optimal conditions and settings of these variables were required for effective separation of particles. Variable factors are discussed below.

4.4.1 Magnetic core material

Proper selection of core material was required to perform material sorting experiments. Core material was selected depending on the frequency required for the sorting experiments. The main objective of the core is to produce a higher magnetic field at the given frequency of operation. A laminated silicon steel core performed better at lower
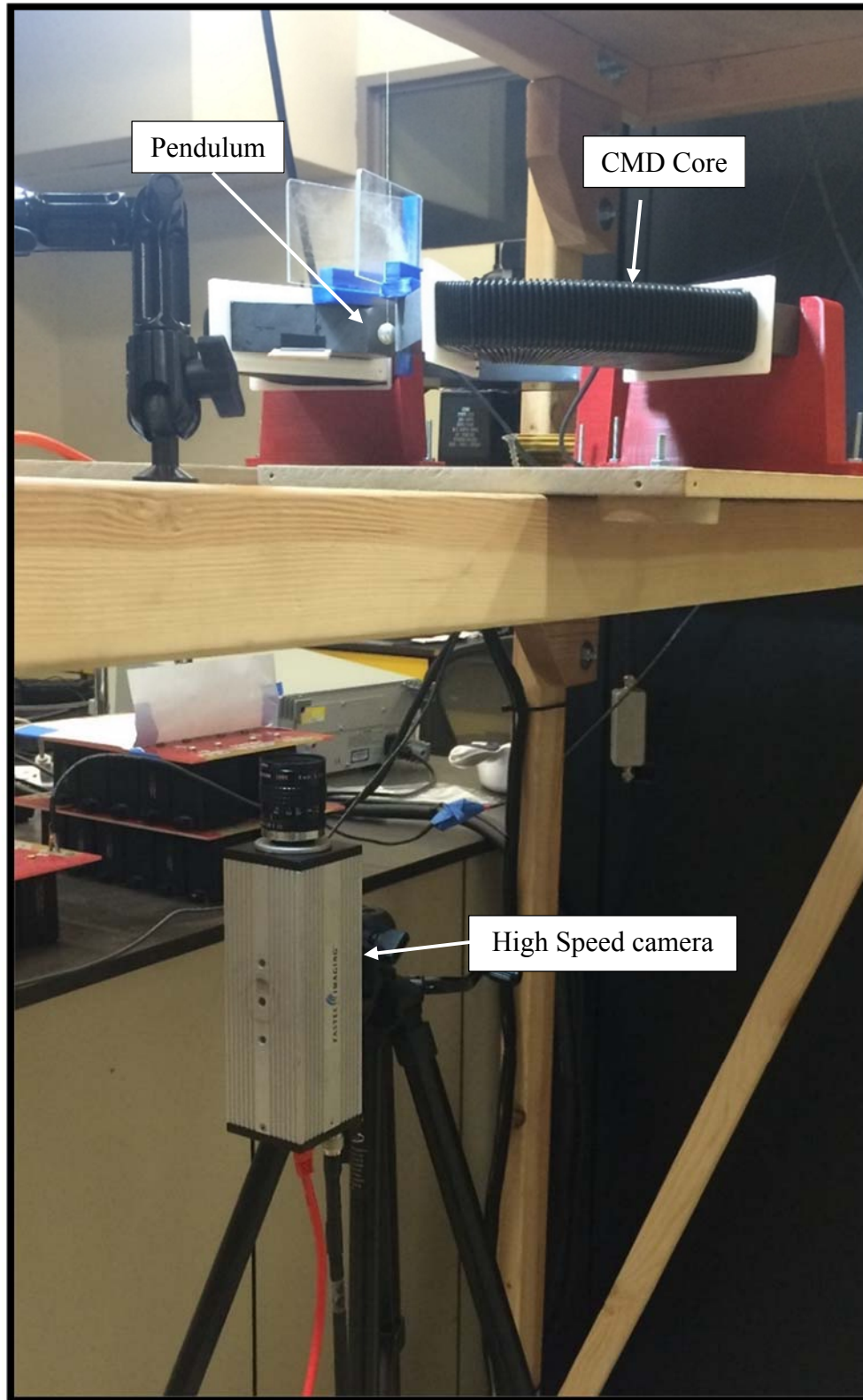
Figure 4.9 Pendulum experiment setup (Photograph © Nakul Dholu 2016)

frequency but at higher frequencies, these cores suffered high eddy current losses induced in the core which resulted in high temperatures in the core material. Ferrite cores were the preferred option to use for high-frequency sorting experiments. Ferrite cores are made by powder metallurgy technique using iron oxide powder blended with other metal oxides and carbonates powders. Ferrite cores experiences lower eddy current losses at higher frequency, have good magnetic permeability, high electrical resistivity, and temperature stability at frequencies ranges from 1 KHz–10 KHz required for the experiments.

4.4.2 Shape of air gap cut

The shape of the cut was a major factor in sorting performance. Magnetic field chooses the path of least resistance in the core and due to that, magnetic field was more concentrated to the apex region of the V-shaped cut. To exert more force on particles during sorting, higher magnetic field intensity must be available at the region where particles were falling into the gap. Also the magnetic field gradient profile through the region of the air gap cut was a critical factor to design the optimal cut geometry. Experiments with silicon steel core and W material ferrite core were done with the regular V-shaped cut while experiments using NiZn ferrite core was done using a double cut. Due to the double-angled cut geometry in NiZn ferrite core, more magnetic field intensity was achieved at the air gap, so lower height of the core was required compared to other cores.

4.4.3 Thermal stability of the core

During operation, the core generates heat due to induced eddy current inside the core material. Due to heat generation, magnetic field intensity at the air gap decreases. So

during extended operation, heat management of the core was required to maintain magnetic field strength. Thermal management of the core during experiments was done using a 12 V DC fan to quickly conduct heat away from the core.

4.4.4 Frequency

Frequency was the most important factor affecting performance of nonferrous material sorting experiments. It was easy to sort nonferrous material with distinct physical and chemical properties compared to alloys with almost similar physical and chemical properties. In both sorting cases, optimal frequency was required to achieve better separation. Optimal frequency was defined as the frequency at which the deflection force of the different materials to be sorted varies from each other, the most. Also, the sorting frequency selection depends on the size of the particles. The smaller the particle size, the higher the frequency is to sort them and vice versa.

4.4.5 Size of the particles

The particle size was a factor to be considered while performing sorting experiments. It was observed that material with similar chemical composition and electrical conductivity experienced varied deflection force at a particular frequency. Larger particles experienced more force than smaller particles. So samples used for sorting experiments were size screened to avoid separation of similar kinds of material during sorting experiments. Results of pendulum experiments also indicated the effect of size of particle on its deflection force. Also, due to size and geometry of the air gap of the core, material sorting was limited to particles smaller than the air gap cut size. It was also observed that

the larger size particles blocked the gap and prevented other particles from entering the gap for sorting and thus resulted in decreasing throughput of the sorting process.

4.4.6 Shape of the particle

The shape of the particles had great influence on sorting performance. Solid spherical-shaped particles were deflected more easily than the flat pieces. Eddy current is induced in a cross-sectional area perpendicular to the direction of the alternating magnetic field. For spheres, area under the circumference is available for eddy current inductions while for nonspherical-shaped particles especially flat pieces, the cross-sectional area perpendicular to external magnetic field depends upon the orientation in which they enter the magnetic field. Hence, for flat shaped pieces, eddy current induction is anisotropic in nature. Research work done at Lulea University of Technology, Sweden (*50*) also showed variation in deflection force on the material with the same chemical and physical properties but difference in shapes. To sort different aluminum alloy coupons, a special adaptor was used to keep the orientation of the coupons by which the maximum cross-sectional area was exposed perpendicular to the alternating magnetic field. So depending on the shape of the particles to be sorted, special feeding techniques were required.

4.4.7 Electrical conductivity of the particles

Deflection of material was highly dependent on the conductivity of the material to be sorted. High conductive material was deflected more than materials with lower conductivity. Alloys have a very narrow range of conductivity difference, so sorting different alloys was difficult compared to sorting two different metals. When material was

physically deformed, electrical conductivity of that material was also decreased.

4.4.8 Density of the particles

Density of the particles was one of the factors associated with a particle's deflection trajectory. Gravitational force acting on the particle tends to change its trajectory downward. So, the greater the density of the particle, a greater downward force is acted on them and resulted in lower horizontal travel away from the air gap of the core.

4.4.9 Feeding height

An opposing force was experienced on the particles when they were delivered to the core gap from the direction opposite to the particle's deflection, so it was the preferred option to feed the particle from a certain height so that opposing force action on the feed particles could be minimized. Increasing the height resulted in lower deflection of the particle due to higher gravitational force acting on the particle. So there was an optimal height at which the best deflection was achieved. Also, smooth feeding of the material into the gap was important.

4.4.10 Grade of the feed material

Recovery of the material after separation was dependent on the grade of the feed material. During the sorting process, two to three materials were simultaneously entering the air gap of the electromagnets and after getting deflected on the way they would sometimes collide with each other, resulting in change from the original deflection trajectory, which then resulted in the particles falling into the wrong collection bin.

CHAPTER 5

EXPERIMENTAL RESULTS AND DISCUSSION

Experiments were performed to collect data to support and understand the capability of solid state variable-frequency eddy current sorting. The first set of experiments performed were to sort nonferrous metals from nonconducting particles followed by a set of experiments to sort a mixture of nonferrous metals and alloys into like metals and alloys. Then, ejection velocity experiments were performed to compare theoretically calculated and actual ejection velocities. Later, experiments were conducted to sort mixtures of different aluminum alloys using optimal sorting frequencies. Finally, experiments were conducted to separate a mixture of aluminum and copper fractions from real-world Zorba scrap.

Initial experiments were performed with the aim to analyze different feeding techniques which can be used in dynamic conditions with minimal changes required to feed different types of materials. Learning from the initial experiments led us to design an overall EDX hardware setup as described in Chapter 4 which was used to perform repeatable experiments at different operating conditions.

5.1 Metal and nonmetal separation

The aim of this experiment was to develop an initial level of confidence in the solid state eddy current separation method. The initial phase of research was performed to separate ~ 6 mm diameter spheres of nonferrous metals mixed with nonconducting ceramic spheres using a ferrite core (0W49740TC) at 6 kHz and 30 mT of B-field. The experiments were performed using individual mixtures of ceramic spheres with aluminum, copper, and brass spheres. Due to monosized feed in all the experiments, the deflection force exerted on the nonferrous spheres was similar and resulted in achieving higher recoveries. Experimental results of individual mixture separations are discussed below.

5.1.1 Aluminum and ceramic mixture sorting

In this experiment, the feed material consisted of 200 pieces of irregular aluminum metal shots with dimensions ~ 6 mm × ~ 6 mm × ~ 3 mm (L×B×T) mixed with 200 pieces of 6 mm diameter spherical ceramic material. Ten consecutive experimental runs were performed to analyze sorting efficiency at 6 kHz and also at optimal position of the collector box. Table 5.1 shows grade and recovery of aluminum separation experiments. From Figure 5.1, the average grade and recovery of aluminum was 99.26% and 100 %, respectively. Due to the similar shape and size of the aluminum material feed, deflection was similar for all of the aluminum particles, hence very high recovery was achieved. Interaction of aluminum particles with the ceramic particles at the core gap due to random collision caused 2 to 4 ceramic spheres to get deflected along with aluminum particles resulting in a slightly lower grade of recovered aluminum. Figure 5.2 shows recovered aluminum particles and ceramic particles after the separation.

Table 5.1 Grade and recovery achieved in metals and nonmetals separation experiments

| Experiment No	Irregular Oval-shaped Solid Aluminum (8 mm x 6 mm x 3 mm)		Irregular Copper (3 mm × 8 mm)		Spherical Brass (6 mm)	
	Grade	Recovery	Grade	Recovery	Grade	Recovery
1	99.01	100.00	94.71	98.50	92.59	100.00
2	99.50	100.00	96.57	98.50	94.34	100.00
3	99.50	100.00	96.08	98.00	91.74	100.00
4	100.00	100.00	96.10	98.50	92.59	100.00
5	99.01	100.00	95.15	98.00	91.32	100.00
6	99.01	100.00	96.06	97.50	93.90	100.00
7	100.00	100.00	95.59	97.50	92.17	100.00
8	98.52	100.00	96.08	98.00	89.29	100.00
9	98.52	100.00	98.00	98.00	90.91	100.00
10	99.50	100.00	96.53	97.50	93.46	100.00
Mean	**99.26**	**100.00**	**96.09**	**98.00**	**92.23**	**100.00**
Std Dev	**0.50**	**0.00**	**0.84**	**0.39**	**1.43**	**0.00**
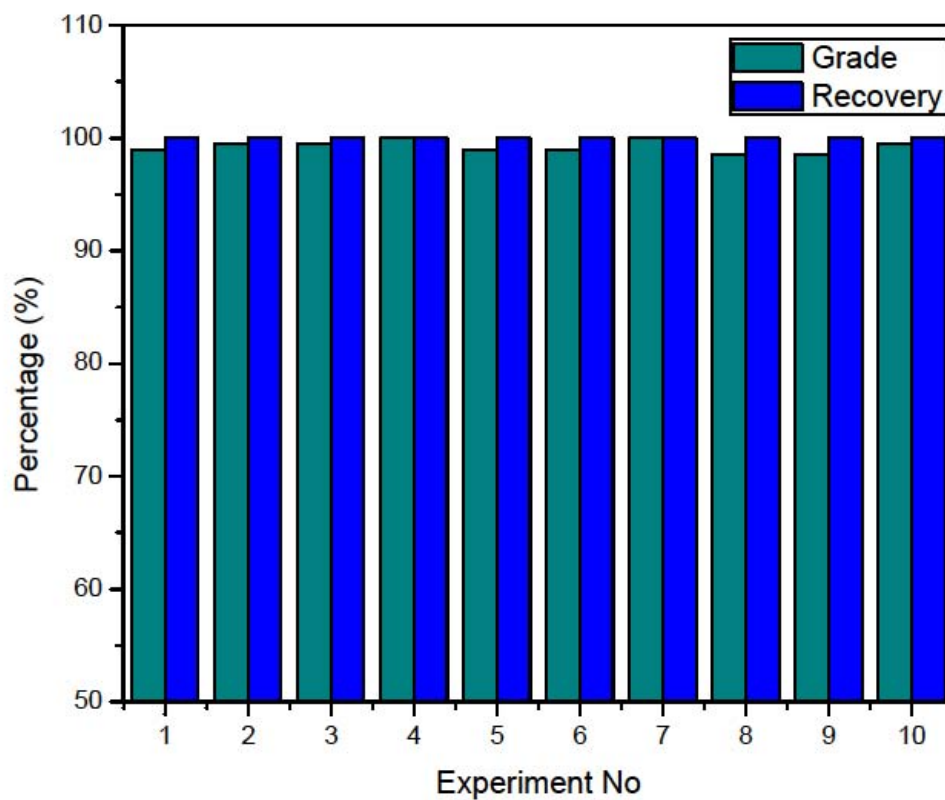
Figure 5.1 Grade and recovery of aluminum achieved in ten consecutive runs of separation experiments

Figure 5.2 Aluminum (left) and ceramic spheres (right) after separation (Photograph © Nakul Dholu 2016)

5.1.2 Copper and ceramic mixture sorting

For the copper separation experiment, the feed material was made by mixing 200 pieces of irregularly shaped copper shots having dimensions in the range of ~3 mm to ~ 6 mm and 200 pieces of 6 mm diameter spherical ceramic material. Separation was performed at 6 kHz and the collector bin was placed close to the core compared to the bin position used for aluminum separation because the horizontal deflection of the nearly same sized copper was less than aluminum. Grade and recovery results of copper separation is shown in Table 5.1. Average grade and recovery of copper was 96% and 98%, respectively. Individual grade and recovery achieved in each experiment is shown in Figure 5.3. Due to the bin position being close to the core, the probability of ceramic spheres getting deflected to the copper bin due to random collision was greater, and hence, resulted in a lower grade for sorted copper. Figure 5.4 shows recovered copper particles after the separation.

5.1.3 Brass and ceramic mixture sorting

In this experiment, the feed material consisted of 200 pieces of 6 mm diameter brass spheres mixed with 200 pieces of 6 mm diameter spherical ceramic material. Ten consecutive experimental runs were performed to analyze sorting efficiency at 6 kHz. Position of collection was even closer to the core compared with aluminum and copper separation experiments which resulted in more numbers of ceramics spheres getting collected into brass bins due to random collision taking place during separation. Table 5.1 shows grade and recovery of brass separation experiments. In Figure 5.5, the average grade and recovery of brass was 92% and 100% respectively. Figure 5.6 shows 100%, recovered brass particles after the separation.

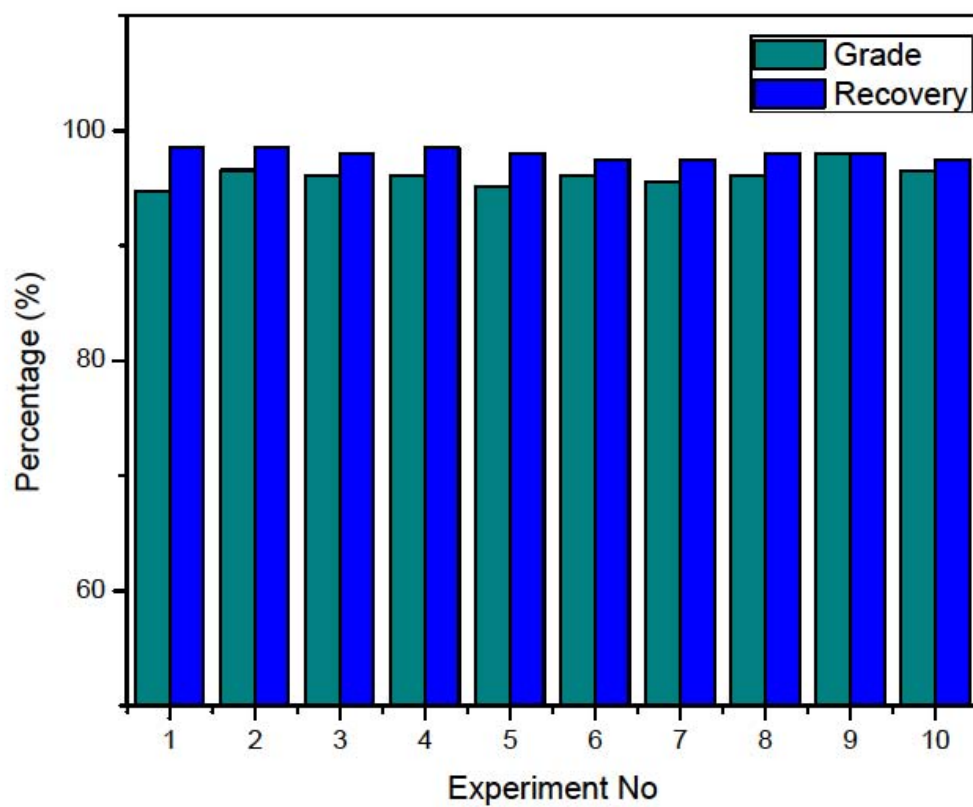Figure 5.3 Grade and recovery of copper achieved in ten consecutive runs of separation experiments
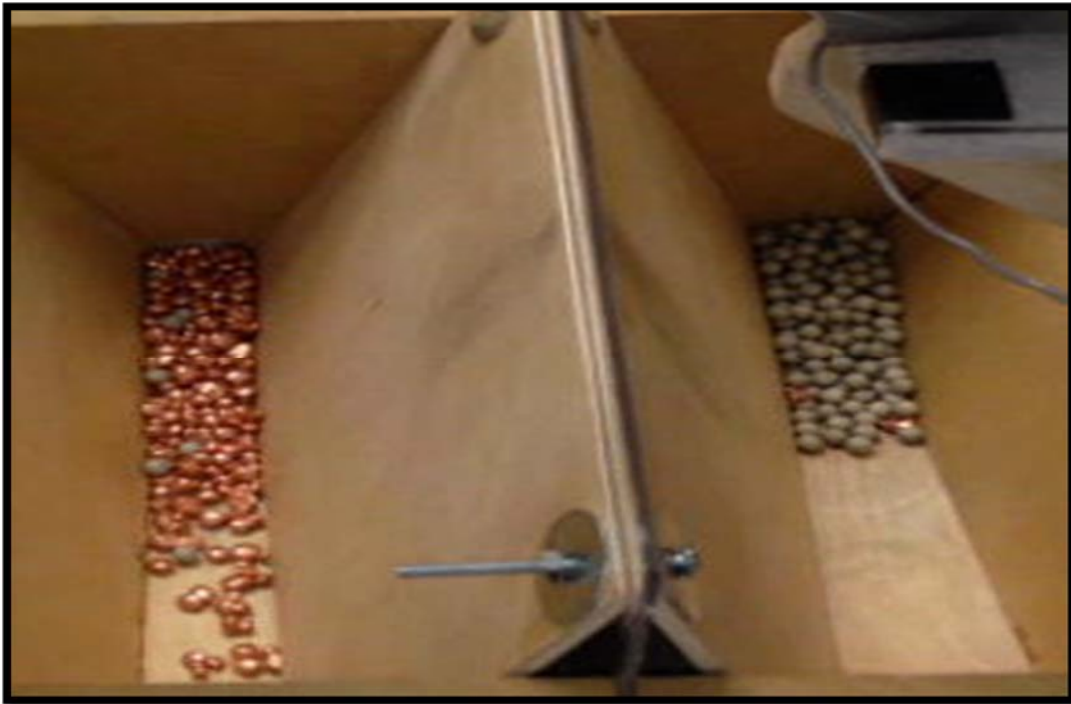
Figure 5.4 Copper (left) and ceramic spheres (right) after separation (Photograph © Nakul Dholu 2016)
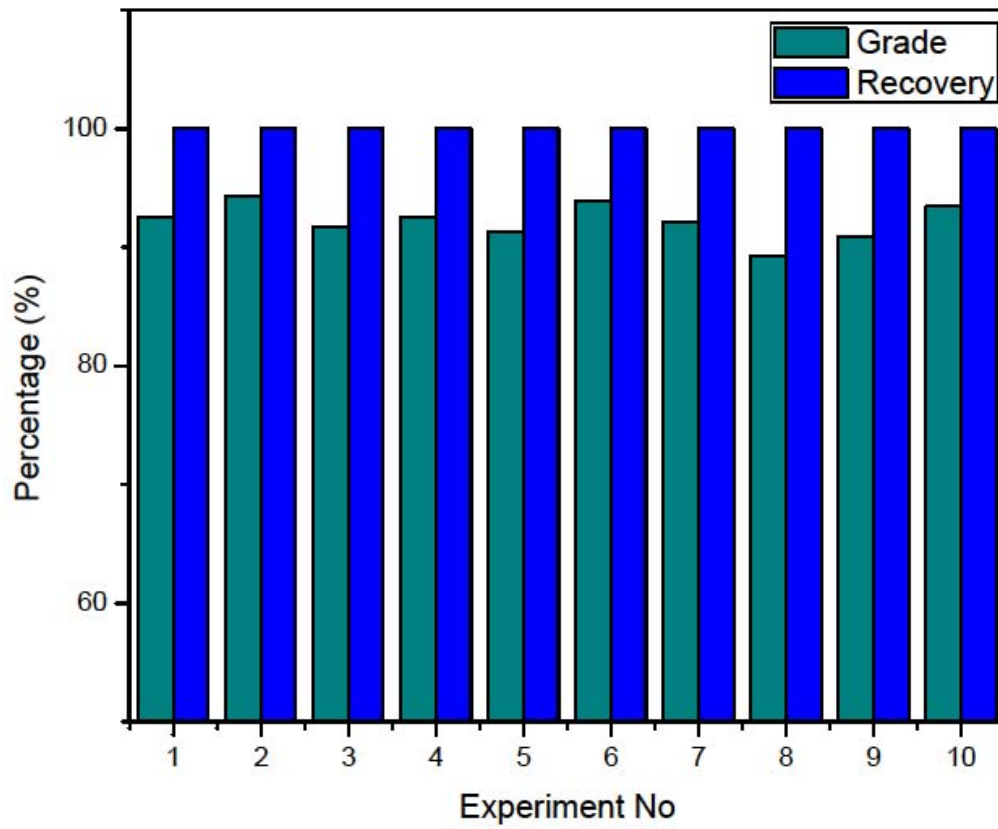
Figure 5.5 Grade and recovery of brass achieved in ten consecutive runs of separation experiments

Figure 5.6 Brass (left) and ceramic spheres (right) after separation (Photograph © Nakul Dholu 2016)

5.2 Metals and alloy sorting experiments

This experiment was conducted to determine the capability of the EDX to separate different metals anrd alloys from one another. Separation of metals and alloys from non-conducting particles was easily achievable as discussed in previous selections, but to sort metals and alloys from each other, an optimal sorting strategy is required. For an optimal sorting strategy, separation of individual metals or alloy fractions is performed at a particular frequency.

In these experiments, the feed material consisted of 200 pieces of 6 mm diameter spheres of aluminum, copper, brass, and Titanium 6-4 each. A double stacked ferrite core (0W49740TC) was used for these experiments. As shown in Figure 5.7, sorting was performed in three stages where the aluminum fraction was recovered in stage one, the Titanium 6-4 fraction was recovered in stage two, and copper and brass fractions were separated in stage three. Ten consecutive runs were performed to analyze grade and recovery achieved. Individual sorting stages are described in detail in the next section.

5.2.1 Optimal sorting strategy: stage 1 aluminum recovery

The first stage of these experiments were performed at 6.5 kHz to recover aluminum material fractions from the rest. Due to their high electrical conductivity aluminum spheres deflected the farthest so, the collector box was positioned to collect aluminum fractions in the far bin while the rest of the fractions were collected into the near bin as shown in Figure 5.8. According to Table 5.2, average grade and recovery of aluminum fraction was 98% and 98%, respectively. Grade and recovery of sorted aluminum achieved in each experiment is shown in Figure 5.9.
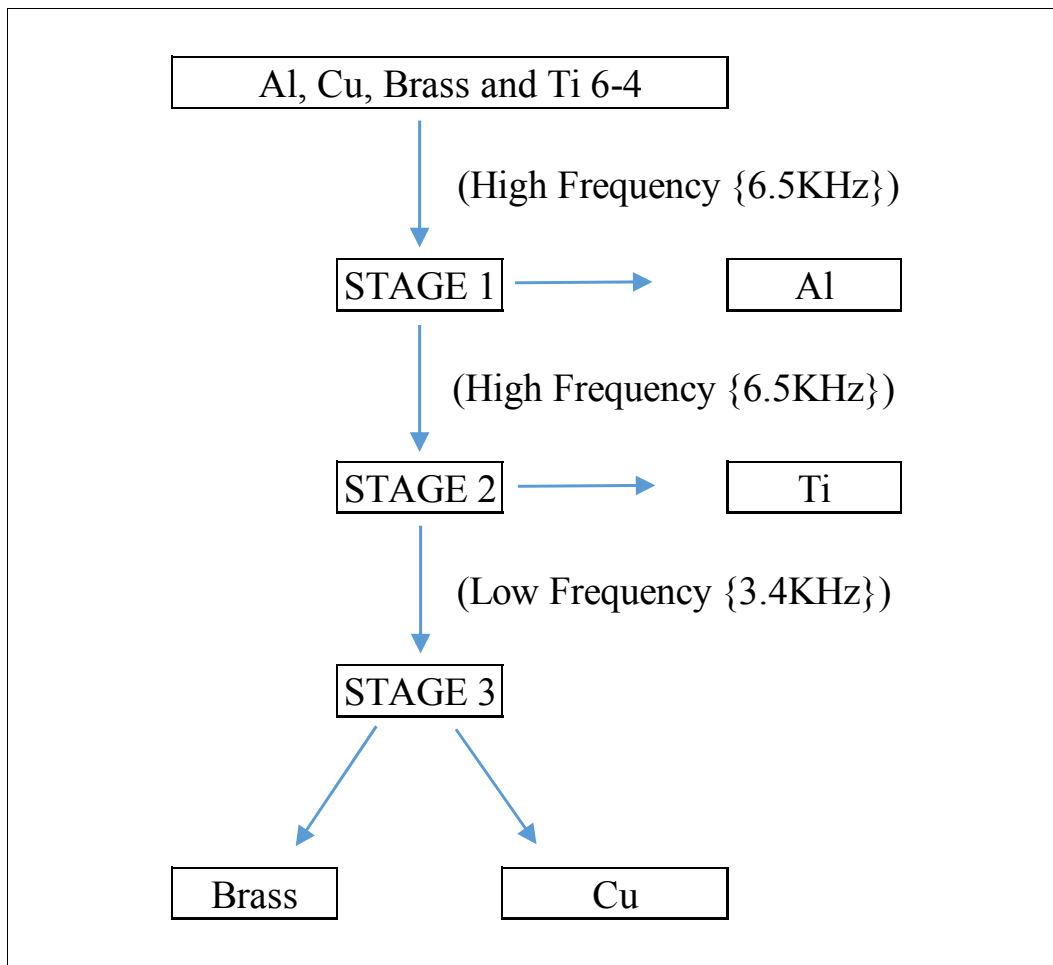
Figure 5.7 Optimal sorting strategy to separate aluminum, copper, brass and Titanium 6-4

Figure 5.8 Optimal sorting experiments of metals and alloys: aluminum fraction (right) and remaining fractions (left) stage 1 separation (Photograph © Nakul Dholu 2016)

Table 5.2 Grade and recovery achieved in metals and alloys separation experiments

11	Al		Cu		Brass		Ti 6-4	
	Grade	Recovery	Grade	Recovery	Grade	Recovery	Grade	Recovery
1	94%	100%	98%	93%	97%	97%	98%	98%
2	96%	100%	98%	96%	99%	99%	100%	99%
3	99%	99%	97%	99%	98%	98%	100%	98%
4	99%	100%	98%	99%	98%	98%	99%	99%
5	99%	99%	98%	99%	97%	98%	98%	97%
6	99%	98%	98%	99%	96%	97%	97%	96%
7	99%	98%	97%	99%	96%	98%	99%	97%
8	98%	98%	98%	97%	96%	100%	99%	97%
9	100%	96%	95%	100%	97%	97%	98%	98%
10	100%	94%	93%	100%	98%	95%	96%	99%
Average	98%	98%	97%	98%	97%	97%	99%	98%
STD Dev	2%	2%	2%	2%	1%	1%	1%	1%

Figure 5.9 Grade and recovery of aluminum fraction achieved in ten consecutive runs of optimal sorting experiment stage 1 separation

5.2.2 Optimal sorting strategy: stage 2 Titanium 6-4 recovery

Titanium 6-4 spheres were recovered in stage 2. This sorting experiment was also performed at 6.5 kHz. Because of lower electrical conductivity of Titanium 6-4, it was deflected the least, hence, the collector bin was placed very close to the core to collect the Titanium 6-4 fraction in the near bin while copper and brass fractions were collected in the far bin as shown in Figure 5.10. Table 5.2 shows the average grade and recovery of Titanium 6-4 fraction was 98% and 97%, respectively. Figure 5.11 shows grade and recovery of Titanium 6-4 fraction achieved in each experiment.

5.2.3 Optimal sorting strategy: stage 3 copper and brass recovery

In the last stage of the optimal sorting strategy experiments, the remaining fraction of the material, copper and brass fractions, were separated and recovered. These separation experiments were performed at 3.4 kHz which was a lower frequency than the previous stages. At higher frequency, horizontal deflection of copper and brass spheres was similar, so no separation was achieved at higher frequency. Lowering the frequency revealed a wide difference in horizontal deflection between copper and brass spheres. The copper fraction was collected in the far bin while brass fractions was collected in the near bin, as shown in Figures 5.12. Per Table 5.2, the average grade and recovery of the copper fraction was 97% and 98%, respectively while average grade and recovery of brass fraction was 97% and 97%, respectively. Figure 5.13 and 5.14 show grade and recovery for copper and brass achieved in individual experiments.

Figure 5.10 Optimal sorting experiments of metals and alloys: Titanium 6-4 fraction (left) and remaining fractions (right) stage 2 separation (Photograph © Nakul Dholu 2016)
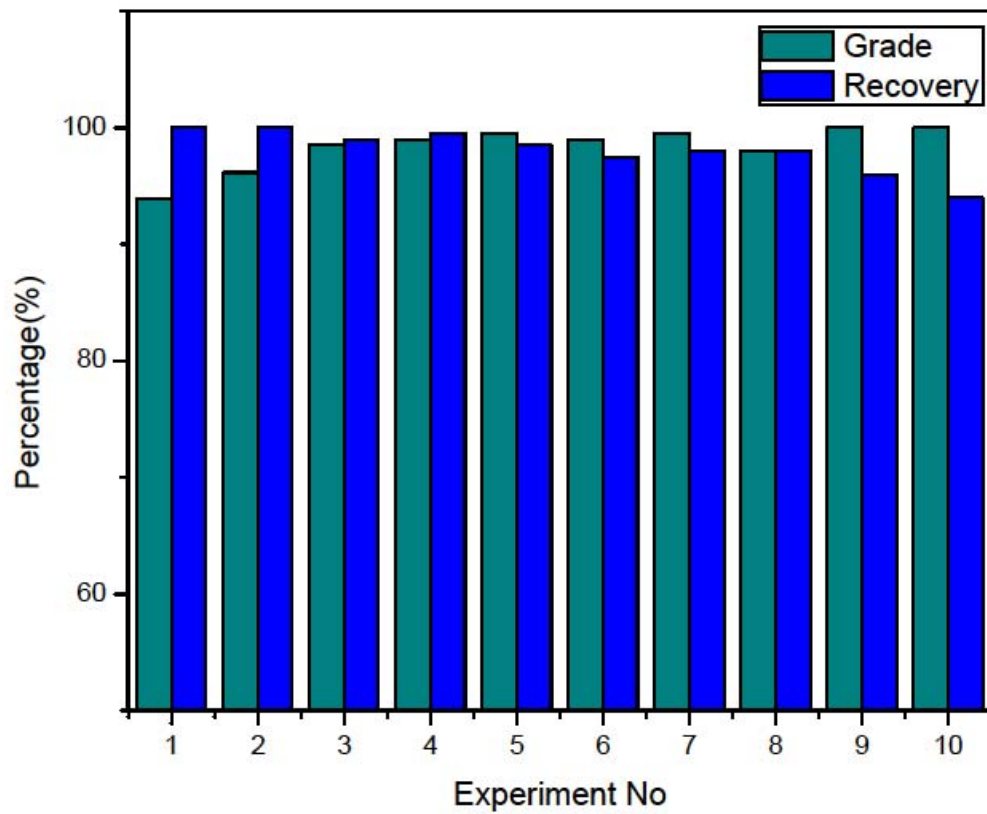
Figure 5.11 Grade and recovery of Titanium 6-4 fraction achieved in ten consecutive runs of optimal sorting experiment stage 2 separation

Figure 5.12 Optimal sorting experiments of metals and alloys: copper fraction (right) and brass fraction (left) stage 3 separation (Photograph © Nakul Dholu 2016)
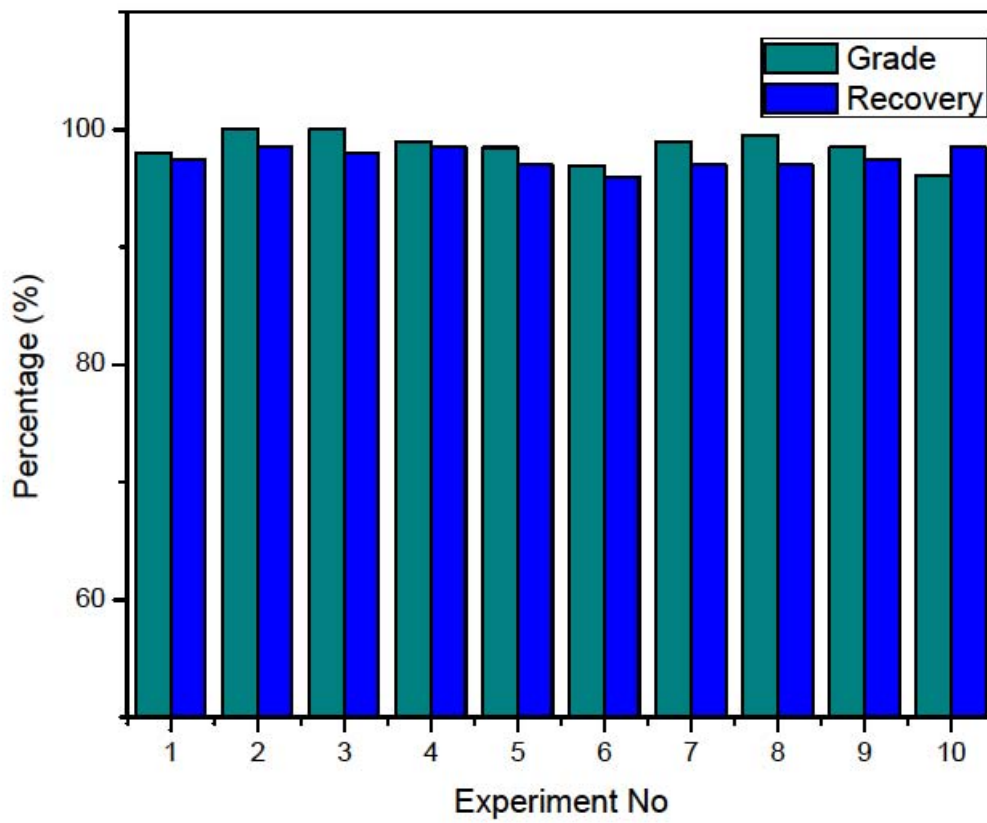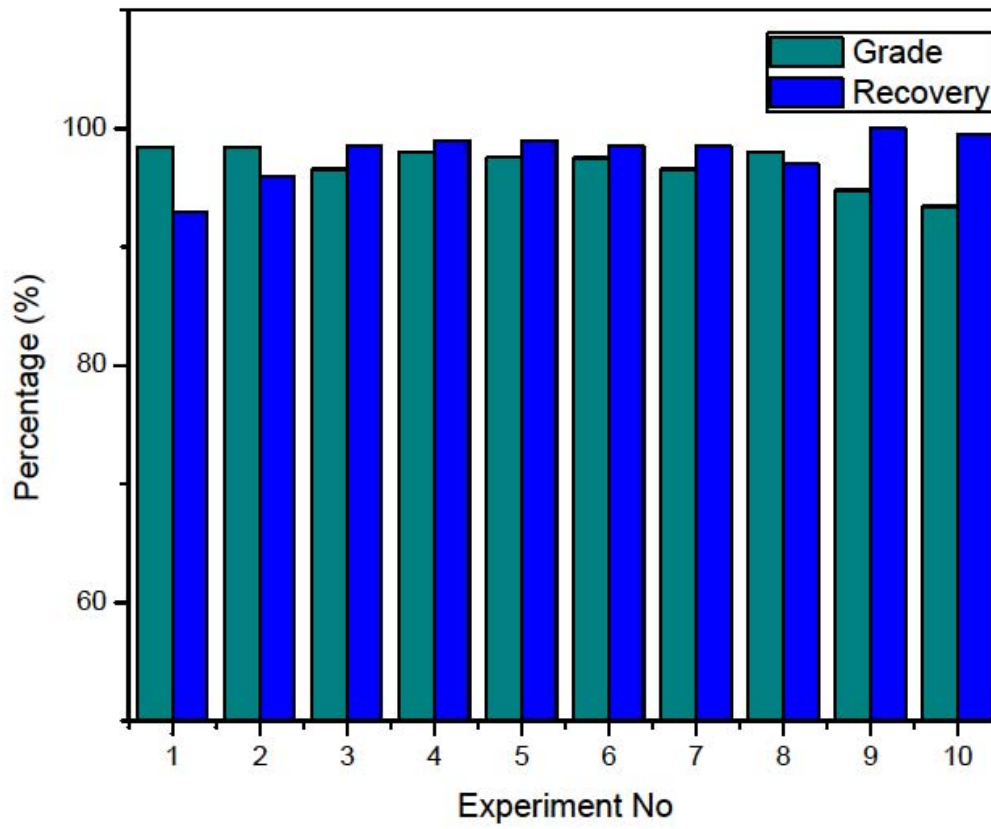
Figure 5.13 Grade and recovery of copper fraction achieved in ten consecutive runs of optimal sorting experiment stage 3 separation
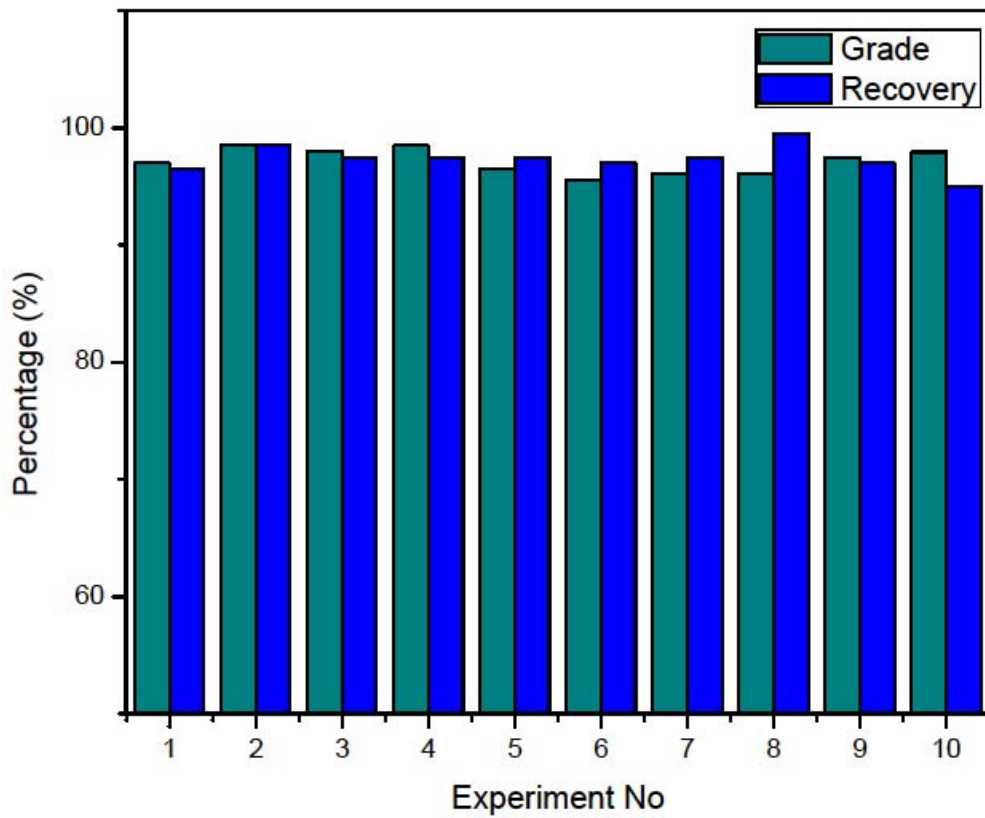
Figure 5.14 Grade and recovery of brass fraction achieved in ten consecutive runs of optimal sorting experiment stage 3 separation

5.3 Pendulum experiments

The purpose of these experiments was to measure the actual ejection velocity of different materials and to compare the results with theoretical ejection velocities calculated using Lohofer's equation, discussed in Chapter 3. Also, this experiment was aimed at understanding the effect of frequency and size on deflection velocity for different materials. Experiments were performed on spheres of different sizes of aluminum, copper, brass, and Titanium 6-4 at different frequencies ranging from 1 kHz to 8 kHz using a Ni-Zn ferrite core. A list of all the experimental parameters and operating conditions are shown in Table 5.3. To minimize discrepancies on operational parameters while performing experiments at a particular frequency on different material sizes and type, the position of all of the spheres was carefully adjusted to maintain constant B-field when the magnet was energized. Results of individual experiments are discussed in the next section.

5.3.1 Ejection velocity calculation experiments for aluminum spheres

Ejection velocity experiments for different sized aluminum spheres were performed at different frequencies. It was observed that aluminum particles experienced high ejection velocity at higher frequency while lower ejection velocity was observed at lower frequency. Table 5.4 shows experimentally calculated ejection velocity results were almost equal to theoretically calculated velocities. Location of all the sphere sizes in all the experiments were kept same, that is, 20 mm away from the inner cut. Ejection velocity results for aluminum spheres are shown on a graphical plot in Figure 5.15.

Table 5.3 Operating parameters and specifications

Parameter	Specification
Frequency (kHz)	8.2, 6.05, 3.95, 1.94, and 0.958 for each size of different material
Material	aluminum, copper, brass, and titanium
Shape of material	Spheres
Diameter (mm)	12, 8, 6, and 4 for each material
B-field (mT)	51 mT at 8.2 kHz
	46 mT at 6.05 kHz and 3.95 kHz
	44 mT at 1.94 kHz and 0.958 kHz
Conductivity (MS/m)	aluminum: 23 MS/m
	copper: 51 MS/m
	brass: 10 MS/m
	titanium 6-4: 0.3 MS/m

Table 5.4 Theoretical and actual ejection velocity calculation for aluminum spheres

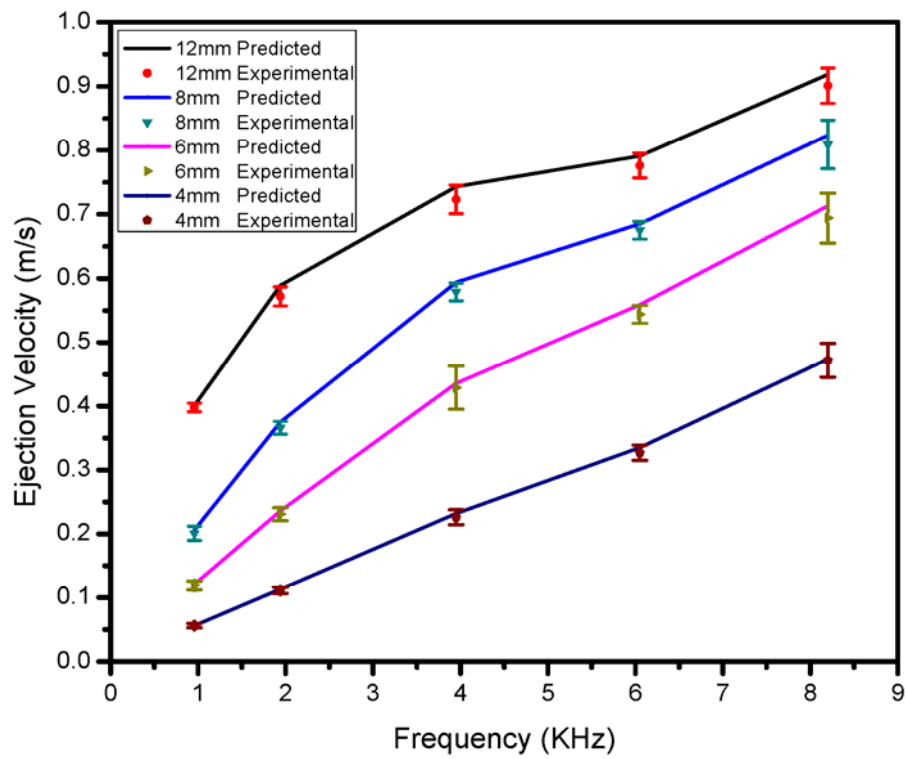| Frequency (KHz)	Ejection Velocity (m/s)			
	12mm		8mm	
	Predicted	Actual	Predicted	Actual
8.200	0.918	0.901	0.8235	0.809
6.050	0.791	0.776	0.685	0.675
3.950	0.743	0.723	0.594	0.579
1.940	0.589	0.572	0.375	0.366
0.958	0.401	0.398	0.206	0.201
Frequency (KHz)	6mm		4mm	
	Predicted	Actual	Predicted	Actual
8.200	0.713	0.694	0.474	0.472
6.050	0.559	0.544	0.335	0.327
3.950	0.436	0.429	0.232	0.226
1.940	0.236	0.231	0.113	0.111
0.958	0.121	0.119	0.056	0.056

Figure 5.15 Theoretical and actual ejection velocity for aluminum spheres

5.3.2 Ejection velocity calculation experiments for copper

This experiment was performed to calculate ejection velocity at different frequencies on different sized copper spheres. Table 5.5 shows the results of calculated ejection velocity. It was observed that larger sized copper spheres tend to deflect more than smaller sized spheres at a given frequency. Ejection velocity of copper spheres was lower than aluminum spheres at higher frequencies but less difference was observed at lower frequency. Figure 5.16 shows the graphical plot of ejection velocity results.

5.3.3 Ejection velocity calculation experiments for brass

The purpose of this experiment was to determine actual ejection velocity of different sizes of brass spheres at different frequencies. Table 5.6 shows that the ejection velocity of brass was lower than aluminum and copper. Due to its lower electrical conductivity, brass tends to deflect less compared to materials with higher electrical conductivity. No deflection was observed on smaller sized brass spheres at lower frequency. A graphical plot of ejection velocity results for brass is shown in Figure 5.17.

5.3.4 Ejection velocity calculation experiments for titanium

Experiments were performed to determine ejection velocity of different sized Titanium 6-4 spheres at different frequencies. Due to the lower electrical conductivity of Titanium 6-4, deflection was only observed on 12 mm spheres at 8.2 kHz and 6.05 kHz. While other spheres showed no deflection, It was concluded that higher frequency was required to cause deflection in titanium.

Table 5.5 Theoretical and actual ejection velocity calculation for copper spheres

Frequency (KHz)	Ejection Velocity (m/s)			
	12mm		8mm	
	Predicted	Actual	Predicted	Actual
8.200	0.537	0.509	0.504	0.494
6.050	0.469	0.456	0.434	0.423
3.950	0.453	0.440	0.407	0.395
1.940	0.396	0.388	0.322	0.315
0.958	0.336	0.331	0.218	0.218
Frequency (KHz)	6mm		4mm	
	Predicted	Actual	Predicted	Actual
8.200	0.470	0.466	0.393	0.387
6.050	0.397	0.386	0.309	0.303
3.950	0.356	0.348	0.242	0.237
1.940	0.242	0.237	0.131	0.130
0.958	0.139	0.136	0.067	0.066
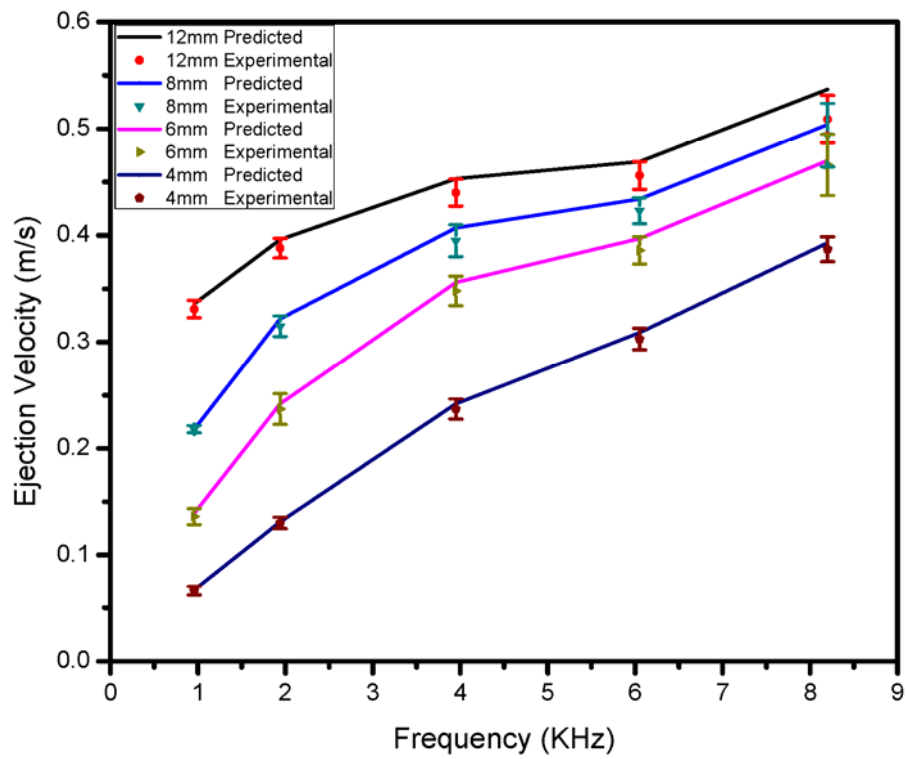
Figure 5.16 Theoretical and actual ejection velocity for copper spheres

Table 5.6 Theoretical and actual ejection velocity calculation for brass spheres

| Frequency (KHz)	Ejection Velocity (m/s)			
	12mm		8mm	
	Predicted	Actual	Predicted	Actual
8.200	0.464	0.452	0.362	0.354
6.050	0.387	0.376	0.274	0.267
3.950	0.336	0.324	0.204	0.198
1.940	0.213	0.208	0.105	0.103
0.958	0.117	0.115	No Deflection	
Frequency (KHz)	6mm		4mm	
	Predicted	Actual	Predicted	Actual
8.200	0.26	0.256	0.136	0.134
6.050	0.183	0.18	0.091	0.089
3.950	0.126	0.122	0.06	0.059
1.940	0.061	0.06	No Deflection	
0.958	No Deflection			
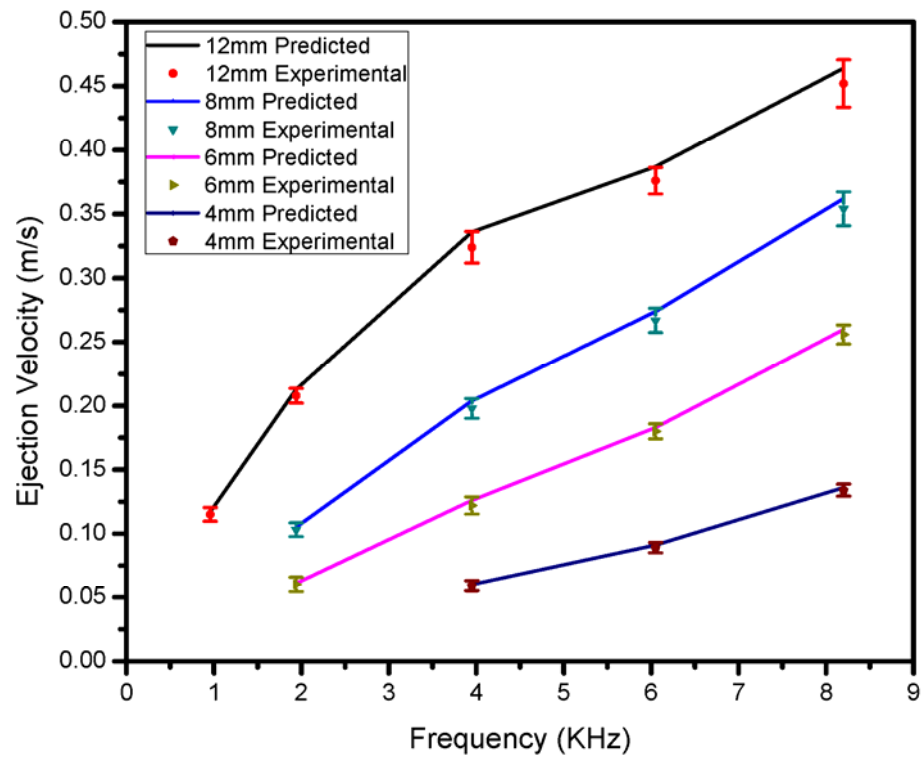
Figure 5.17 Theoretical and actual ejection velocity for brass spheres

5.3.5 Ejection velocity profiles

It was observed from the various pendulum experiment results discussed in section 5.3.2 that the experimentally calculated ejection velocity for spherical-shaped materials has a good fit with the theoretically calculated ejection velocity. This gives us confidence to use Lohofer's equation for predicting ejection velocity of spherically-shaped materials of different sizes at different frequencies. Based on Lohofer's equation, velocity profiles ranging from 1-100 kHz were made for aluminum, copper, brass, and Titanium 6-4 for 12 mm, 6 mm, and 3 mm diameter spheres. Figures 5.18, 5.19, and 5.20 show graphs of velocity profiles for 12 mm, 6 mm, and 3 mm materials. These velocity profiles can be used to determine the optimal frequency required to sort two different materials. Optimal frequency is defined as the minimum frequency where the difference between ejection velocities is enough to collect them into separate collection bins with higher recovery. Velocity profiles shown in Figures 5.18 to 5.20 also show that higher frequency is required to sort smaller sized particles while larger sized particles can be separated at lower frequencies.

Ejection velocity depends on the orientation of the material in the alternating magnetic field. Orientation does not matter for spherical-shaped nonferrous materials as they are always symmetrically oriented to the alternating magnetic field. Hence, velocity profiles discussed in these results are more valid and applicable for spherically-shaped nonferrous materials only.
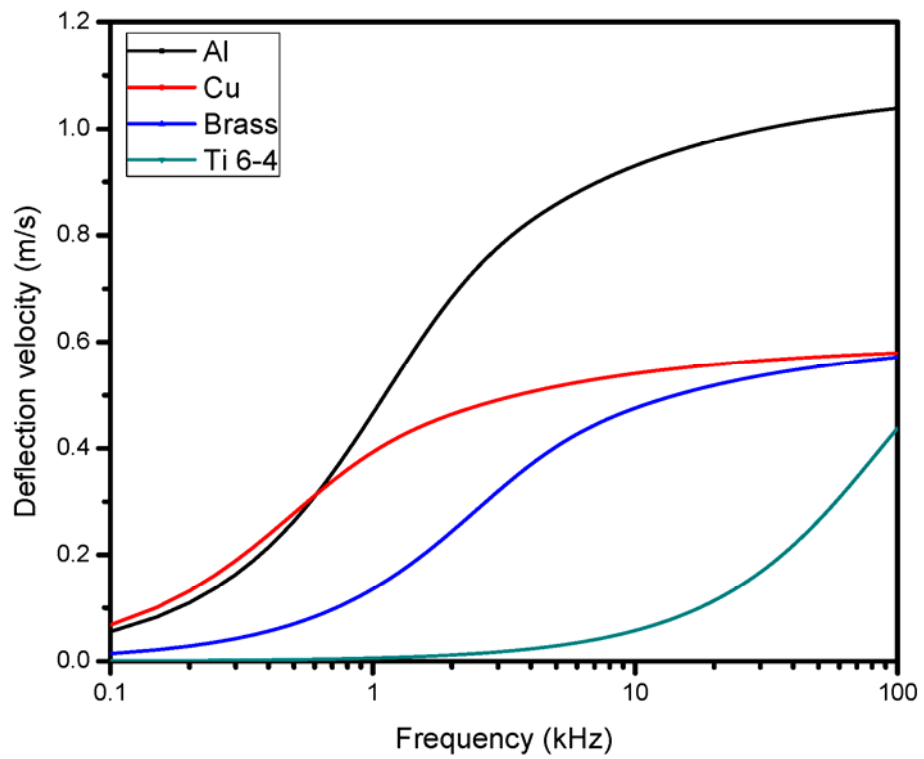
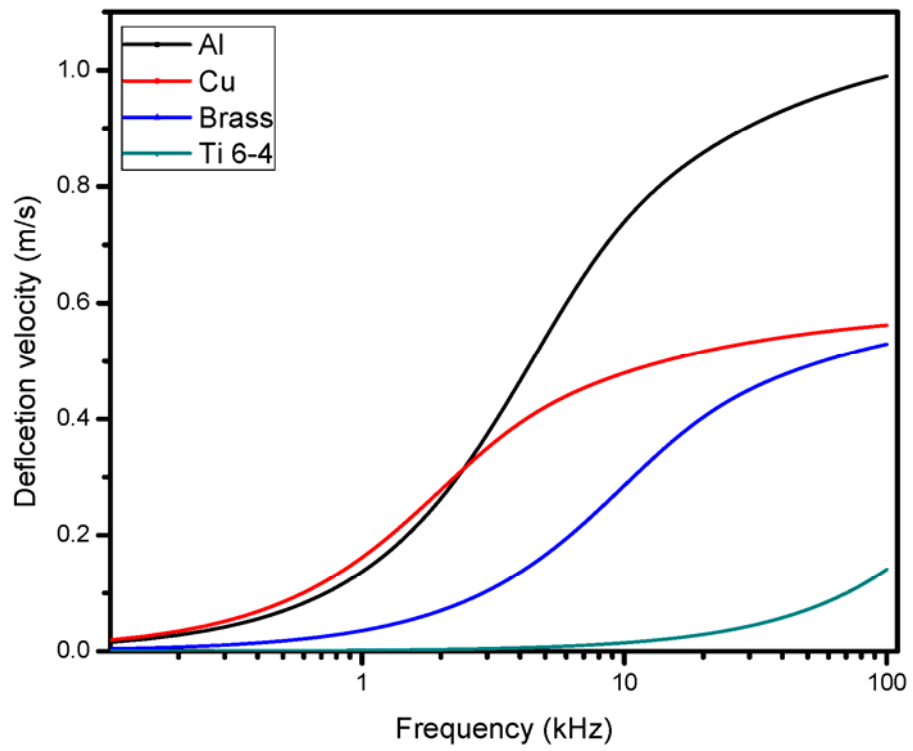Figure 5.18 Ejection velocity of 12 mm spheres at different frequencies

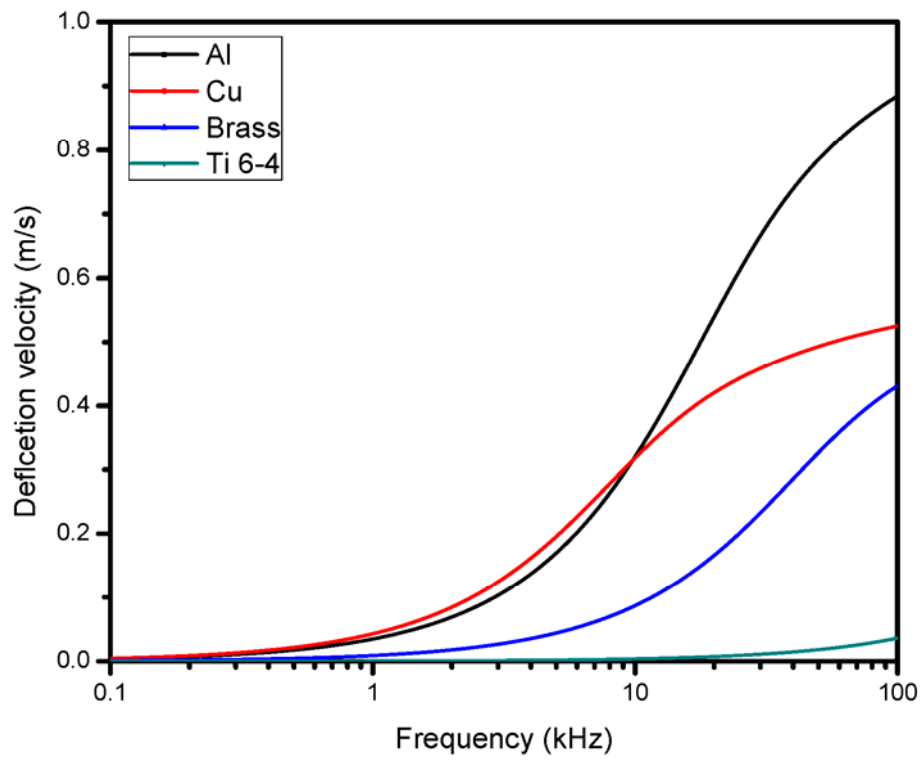Figure 5.19 Ejection velocity of 6 mm spheres at different frequencies

Figure 5.20 Ejection velocity of 3 mm spheres at different frequencies

5.4 Aluminum alloy sorting experiments

These experiments were intended to understand the capability of solid state EDX technology to sort like metal alloys. These experiments were conducted to separate nine different aluminum alloys which are commonly used in automobile and aerospace industries. Based on differences in electrical conductivity, aluminum alloys used for the experiments were sorted into four different groups. Table 5.7 shows a list of aluminum coupons used for these experiments along with their electrical conductivities. It was observed that aluminum alloys had the same horizontal deflection at higher frequencies while at lower frequencies, differences in horizontal deflection were observed. So it was understood that lower frequency was required to separate aluminum alloys. Hence, these experiments were performed at a frequency range of 0.5 kHz to 0.8 kHz.

A grain oriented silicon steel core was used for these experiments as it had higher B-field saturation at lower frequencies compared to ferrite cores used to separate different nonferrous metals in previous experiments. So using silicon steel core, higher magnetic field (i.e., 150mT) was available at the gap of the core which proved an added advantage to separate aluminum alloys with conductivity differences of 5 MS/m. This experiment was performed in three different stages where highly electrically conductive aluminum alloys were separated at the far bin in every stage, while more weakly electrically conducting alloys collected in near bin were used in the next stage for further separation. Figure 5.21 shows three stage separation experiment where alloys with electrical conductivity above 30 MS/m were separated in stage 1. In stage 2, alloys having electrical conductivity ranging between 25 to 30 MS/m were separated and finally, in stage 3, in the far bin alloys with electrical conductivity ranging from 25 to 20 MS/m while in the near

Table 5.7 List of aluminum coupons used for alloy sorting experiments

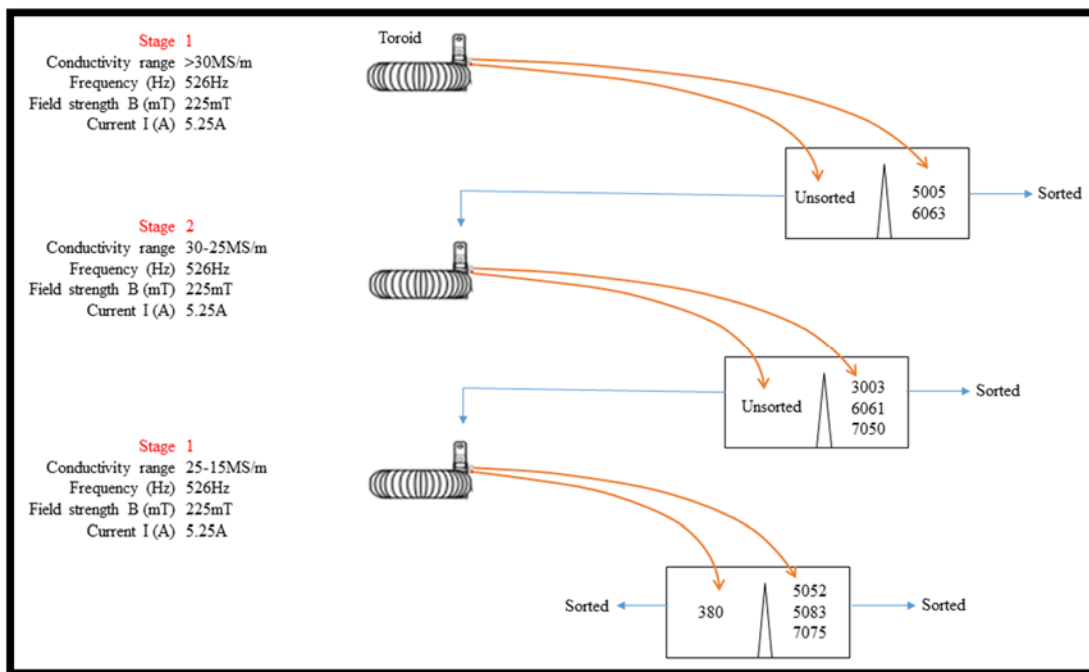| List of Aluminum alloy to be sorted					
Sr No	Alloy	No of coupons	Total weight (g)	average weight of coupon (g)	Conductivity (10^6 S/m)
1	380	25	115.20	4.6	13.73
2	5083	24	91.60	3.8	16.42
3	7075	30	121.10	4.0	18.49
4	5052	30	113.40	3.8	20.39
5	7050	25	117.00	4.7	23.41
6	6061	30	113.10	3.8	25.25
7	3003	30	115.10	3.8	25.55
8	5005	25	98.80	4.0	30.7
9	6063	25	109.40	4.4	32.62
Total			994.70		

Figure 5.21 Aluminum alloy sorting strategy

bin, 300 series cast aluminum alloys with conductivity less than 20 MS/m were separated. Table 5.8 and 5.9 show results of aluminum alloy sorting experiments. It was observed that recovery of higher electrically conductive alloys was 98%, recovery for upper-medium and lower-medium conductive alloys was 86%, and recovery for lower conductive alloys was 71%. Graphical representation of grade and recovery is shown in Figure 5.22. The recovery results clearly indicate potential of the EDX technique to sort aluminum alloys.

5.5 Zorba sorting experiments

Finally, experiments were conducted to sort actual nonferrous scrap material. Zorba scrap was used for this experiment which consists mainly of aluminum and copper fractions. Zorba scrap was irregular in shape and size. This experiment was performed at 7.5 kHz frequency using a Ni-Zn ferrite core. The B-field during the experiment was 50 mT. Zorba scrap was first size screened to recover scrap between 8 mm and 12 mm to prepare feed for the experiment. To analyze sorting performance at different feed grade conditions and to replicate dynamic condition of actual feed grade in real world scrap sorting operations, three sets of feed samples were prepared as shown in Table 5.10. Figure 5.23 shows a zorba feed sample with grade of aluminum and copper fractions of 65% and 35%, respectively. Sorting results are shown in Table 5.11, overall recovery of aluminum and copper fractions was above 84% and 86%, respectively, and separated material is shown in Figure 5.24. The reason for the lower recovery achieved in real scrap compared to previously discussed results for sorting spherical materials was the size and shape of real scrap particles. It was observed that similar kinds of materials which are non-uniform in size, experienced varied horizontal deflection force. Also, chunky-shaped

Table 5.8 Coupon sorting results

RESULT Expected				RESULT Errors			
Alloy	Mass (g)	% of Total Mass	Conductivity (10^6 S/m)	Alloy	Mass (g)	% of Total Mass	Conductivity (10^6 S/m)
Stage 1				**Stage 1**			
6063	109.4	11.00%	32.62	3003	15.3	1.54%	25.55
5005	94.9	9.54%	30.70	6061	11.3	1.14%	25.25
Stage 2				**Stage 2 Errors**			
3003	99.8	10.03%	25.55	5005	3.95	0.40%	30.70
6061	83	8.34%	25.25	5052	26.4	2.65%	20.39
7050	117	11.76%	23.41	-	-	-	-
Stage 3 Far Bin				**Stage 3 Far Bin**			
5052	83.1	8.35%	20.39	6061	18.8	1.89%	25.25
7075	105	10.56%	18.49	380	32.5	3.27%	13.73
5083	91.6	9.21%	16.42	-	-	-	-
Stage 3 Near Bin				**Stage 3 Near Bin**			
380	82.6	8.30%	13.73	7075	16.1	1.62%	18.49

Table 5.9 Grade and recovery for coupon sorting experiments

Material	Conductivity Range	Grade	Recovery
High Conductivity	35-30 MS/m	88.48%	98.13%
Upper Medium Conductivity	30-25 MS/m	90.81%	86.85%
Lower Medium Conductivity	25-20 MS/m	84.50%	85.77%
Low Conductivity	20-15 MS/m	83.69%	71.70%
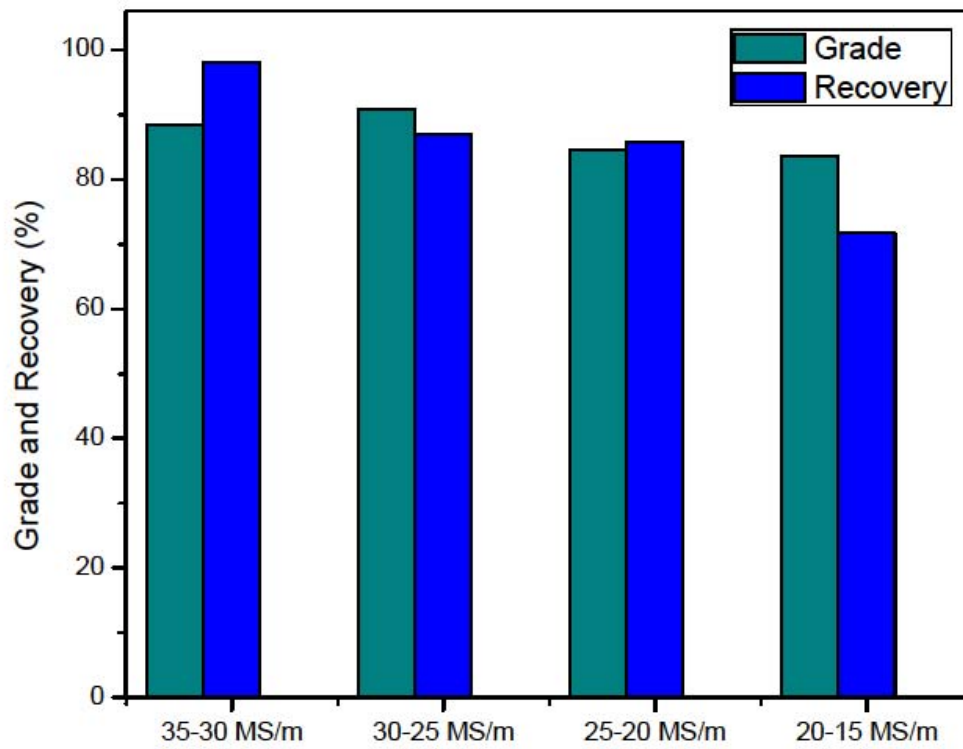
Figure 5.22 Grade and recovery of aluminum alloys sorting

Table 5.10 Zorba feed grade sample sets

Head Grade		
Feed	Al	Cu
Sample set 1	33.82%	66.18%
Sample set 2	44.84%	55.16%
Sample set 3	62.39%	37.61%

Figure 5.23 Zorba scrap feed with 65% aluminum and 35% copper (Photograph © Nakul Dholu 2016)

Table 5.11 Zorba sorting experiment results

Separation run with sample set 1			
Al Rich Bucket		**Cu Rich Bucket**	
Al grade	80.08%	**Al grade**	7.95%
Cu grade	19.92%	**Cu grade**	92.05%
Al recovery	84.92%	**Cu recovery**	89.21%
Separation run with sample set 2			
Al Rich Bucket		**Cu Rich Bucket**	
Al grade	85.25%	**Al grade**	6.16%
Cu grade	14.75%	**Cu grade**	93.84%
Al recovery	95.13%	**Cu recovery**	86.62%
Separation run with sample set 3			
Al Rich Bucket		**Cu Rich Bucket**	
Al grade	92.32%	**Al grade**	13.31%
Cu grade	7.68%	**Cu grade**	86.69%
Al recovery	91.50%	**Cu recovery**	86.69%

Figure 5.24 Sorted zorba scrap showing aluminum rich fraction (right) and copper rich fraction (left) (Photograph © Nakul Dholu 2016)

particles experienced more deflection compared to flat plate type shaped particles. Random collision of particles during sorting also contributed in lower recovery rates. With refinements in feeding technique, ferrite core designs, and developing recirculating sorting techniques, recovery of nonferrous metals can be improved.

CHAPTER 6

CONCLUSIONS

The prime objective of this research was to study and analyze the capability of solid state variable frequency eddy current sorting as a technique to separate various nonferrous metals and alloys. The following conclusions can be drawn from the results obtained from the experimental work:

Once the circuit was completely set up, the following steps were followed to excite the coil to resonance to perform eddy current separation experiments.

1. Solid state variable frequency eddy current sorting can easily separate nonferrous metals and alloys mixed with nonconducting materials with high grade and recovery percentages.

2. Mixtures of Al, Cu, Brass, and Titanium 6-4 can be separated into individual fractions in three separation stages when sorted at the optimal frequencies.

3. Pendulum experiments showed that the horizontal deflection of nonferrous material varies with size, frequency, electrical conductivity, and density. The deflection force acting on particles is higher for larger size particles and also at higher frequency, while it is lower for smaller size particles and lower frequencies. Nonferrous metals and alloys with higher electrical conductivity-to-density ratio deflects more compared to materials with a lower ratio

4. Optimal sorting frequency is the frequency where horizontal deflection is large enough to separate two different nonferrous metals or alloys

5. For spheres, the theoretically calculated ejection velocity using Lohofer's equation matches closely with actual ejection velocities. The orientation of a particle in the variable magnetic field determines deflection forces acting on it. Maximum deflection is achieved when the maximum cross section of the area of the particle is exposed perpendicularly to the alternating magnetic field.

6. When exposed to an alternating magnetic field, materials tends to change its orientation to exposes its minimum cross section. This is due to the torque acting of the particle in the presence of a magnetic field.

7. Aluminum alloys can be separated based on the differences in their electrical conductivity. Lower frequency and higher magnetic field are required to separate aluminum alloys.

8. Ferrite material cores with higher B-field saturation and lower resistive loss are best suited for higher frequency operation. Grain oriented cold rolled silicon steel cores are best suited for low frequency operation. Hence, to separate different nonferrous metals and alloys, ferrite cores can be used, and to separate similar metal alloys, silicon steel can be used.

9. Separation of real world Zorba scrap into discrete nonferrous metal fractions can be done using solid state eddy current separation. Variation of Zorba feed grade results in variation in recoveries of individual nonferrous metal fractions. Feed with higher aluminum grade resulted in higher grade and recoveries of separated aluminum and copper fractions.

10. Due to the variability of size and shape in Zorba scrap, lower grade and recoveries were achieved during sorting experiments compared to grade and recovery achieved in separating size controlled spherical materials.

The scope of future work should be to understand and unveil yet the unknown potential of this technology. Cores with better properties and gap geometry should be tested to improve efficiencies of real-world scrap separation. Systems to achieve higher frequency operation should be developed to separate particles smaller than 1 mm. Research on different feeding techniques should be performed to improve grade and recovery. Efforts should be focused to scale up the technology to handle higher feed rates required for industrial operation. These future studies can led to improvements in making efficient solid state eddy current sorters capable of separating a wide range of nonferrous metals and alloy materials.

REFERENCES

1. Mike, R.; John, M. Recycling Twist Cuts Ford Truck Costs. *The Wall Street Journal* [Online], **2014**. http://www. www.wsj.com/articles/how-recycling- shaves-the-cost-of-fords-new-pickup-14187533159 (accessed January 15, 2016).

2. Woollacott, L.C.; Eric, R.H. Mineral and Metal Extraction: An Overview. In *South African Institute of Mining & Metallurgy;* SAIMM: Johannesburg, 1994, M8, pp 412.

3. Joerg, S. Zorba: Small Particles Big Opportunities. *Waste Management World* [Online], **2014**. https://waste-management-world.com/a/zorba-small-particles-big-opportunities (accessed January 15, 2016).

4. Dalmijn, W.L. In *Practical Applications of Eddy Currents in the Scrap Recycling,* Proceeding of the Second International Symposium Recycling of Metals and Engineering Materials, Williamsburg, VA, USA, Oct 28-31,1990; Minerals, Metals and Materials Society: Pennsylvania, 1990.

5. Edison, T.A. Ore Separator. U.S. Patent 400,317, March 26, 1889.

6. Halliday, D.; Resnick, R.; Walker, J. *Fundamentals of Physics,* 4th ed.; John   Wiley & Sons, Inc.; Somerset, NJ, 1997; pp 537-570.

7. Schloemann, E. Eddy-current Separator Methods. *Prog. Filt. Sep. Technol.* **1979**, *1*, 29–82.

8. Edison, T. A. Ore Separator. U.S. Patent 400,317, March 26, 1889.

9. Maxim, H. S. Magnetic Separator. U.S. Patent 402,684, May 7, 1889.

10. Moffatt, R. R. Electro-magnetic Separator. U.S. Patent 411, 899, October 1, 1889.

11. Isbell, H. L. Polyphase Magnetic Separator. U.S. Patent 1,066,619, July 8, 1913.

12. Mordey, W. M. Electromagnetic Separation or Concentration of Minerals. U.S. Patent 1,729,589, September 14, 1929.

13. McCarthy, J. B. Concentrator. U.S. Patent 1,417,189, May 23, 1922.

14. Benson, W. H.; Falconer, T. H. Electrodynamic Separator. U.S. Patent 3,448,857, June 10, 1969.

15. British Thompson-Houston Co. Improvements in and Relating to the Electromagnetic Separation of Complex Ores. British Patent 305,102, December 19, 1929.

16. Lee, R. Ore Concentrator. U.S. Patent 1,829,565, October 27, 1931.

17. Lovell, W. V. Electromagnet. U.S. Patent 2,400,869, May 28, 1946.

18. Benowinz, S. Magnetic Pulley for Removal of Non-magnetic Pieces from Waste Material. U.S. Patent 3,892,658, July 1, 1975.

19. Roos, C. E. *Nonferrous Metal Sorting at Vanderbilt University. Final Report to the Solid Waste Management Office*; Environmental Protection Agency: Nashville, TN, 1976.

20. Vanderbilt University. Method and Apparatus for Separation of Conductive Materials by Endless Movement of Magnetic Field. British Patent 1,324,126, May 23, 1973.

21. Vanderbilt University. Method and Apparatus for Separation of Conductive Materials by Endless Movement of Magnetic Field. British Patent 1,324,126, July 19, 1973.

22. Zarkhova, S. M. Method and Apparatus for Electro Dynamic Separation of Nonmagnetic Free-flowing Materials. U. S. Patent, December 9, 1980.

23. Morey, B. W. Separation of Non-magnetic Conductive Metals. U.S. Patent 4,137,156, January 30, 1979.

24. Laithwaite, E. R. Separation of Non-ferromagnetic Metals from Fragmented Material. U.S. Patent 4,459,206, July 10, 1984.

25. Reid, P. T. Separation of Non-magnetic Electrically Conductive Items by Electromagnetic Eddy Current Generation. U.S. Patent 5,064,075, November 12, 1991.

26. Rousseau, M.; Melin, A. Processing of Non-magnetic Fractions from Shredded Automobile Scrap: A Review. *Resour. Conserv. Recycl.* **1989**, *2* (2), 139–159.

27. Dalmijin, W. L.; Houwelingen, J. A. New Developments in the Processing of the Non-ferrous Metal Fraction of Car Scrap. In *Recycling of Metals and Engineered Materials.* Minerals Metals and Materials Society: Warrendale, PA, USA, 1995; pp 739–750.

28. Rem, P. C. *Eddy-current Separation*; Eburon: Delft University of Technology, The Netherlands, 1990.

29. Cui, J.; Forssberg, E. Mechanical Recycling of Waste Electrical and Electronic Equipment: A Review. *J. Hazard. Mater.* **2003**, *99* (3), 243–263.

30. Zhang, S.; Rem, S.; Forssberg, E. The Investigation of Separability of Particles Smaller Than 5 mm by Eddy Current Separation Technology. Part I: Rotating Type Eddy Current Separators. *Magn. Electr. Separ.* **1999**, *9* (4), 233–251.

31. Schloemann, E. Separation of Non-magnetic Metals from Solid Waste by Permanent Magnets-II Experiments on Circular Disks. *J. Appl. Phys.* **1975**, *46* (11), 5022–2029.

32. Braam, B. C.; Van Der Valk, H. J. L.; Dalmijn, W. L. Eddy-current Separation by Permanent Magnets Part II: Rotating Disc Separators. *Resour. Conserv. Recycl.* **1988**, *1* (1), 3–17.

33. Schubert, G. Processing of Scrap and Refuse Containing Non-ferrous Metals—Part 2. *Aufbereit. Tech.* **1991**, *41*, 78.

34. Hans, J. L.; Van Der Valk, H. J. L.; Dalmijn, W. L.; Duyvesten, W. P. P. Eddy-current Separation Methods with Permanent Magnets for the Recovery of Non-ferrous Metals and Alloys. *Erzmetall.* **1998**, *41*, 266–274.

35. Lohofer, G. Theory of Electromagnetically Levitated Metal Sphere I: Absorbed Power. *SIAM J. Appl. Math.* **1989**, *48* (2), 567–581.

36. Woltereck, M.; Ludwig, R.; Michalson, W. A Quantitative Analysis of the Separation of Aluminum Cans Out of Waste Stream Based on Eddy Current Induced Levitation. *IEEE Trans. Magn.* **1997**, *33* (1), 772–781.

37. Rem, P. C.; Leest, P. A.; Van Der Akker, A. J. A Model for Eddy Current Separation. *Int. J. Miner. Proc.* **1997**, *49* (3), 193–200.

38. Rem, P. C.; Beunder, E. M.; Van Der Akker, A. J. Simulation of Eddy Current Separators. *IEEE Trans. Magn.* **1998**, *34* (4), 2280–2286.

39. Fraunholez, N.; Rem, P. C.; Hanser, P. A. Dry Magnus Separation. *Miner. Eng.* **2001**, *15*, 45–51.

40. Lungu, M.; Rem, P. Eddy-current Separation of Small Nonferrous Particles by a Single-disk Separator with Permanent Magnets. *IEEE Trans. Magn.* **2003**, *39* (4), 2001–2067.

41. Lungu, M. Separation of Small Nonferrous Particles Using an Angular Rotary Drum Eddy-current Separator with Permanent Magnets. *Int. J. Miner Proc.* **2005**, *78* (1), 22–30.

42. Saveliev, V. L. System and Method for Separating Electrically Conducting Particles. U.S. Patent 5,772,043, June 30, 1998.

43. Pugh, E. M.; Pugh, E. W. *Principles of Electricity and Magnetism*, 2nd ed.; Addison-Wesley Publishing Company, Inc: Boston, MA, 1060.

44. Jackson, J. D. *Classical Electrodynamics*, 3rd ed.; John Wiley and Sons, Inc.: New York, 1998.

45. Vander Valk, H. J. L.; Braam, B. C.; Dalmijn, W. L. Eddy Current Separation by Permanent Magnets Part I: Theory. *Resour. Conserv. Recycl.* **1986**, *12* (3-4), 233–252.

46. Kim, D. Electrodynamic Separation of Conducting Particles in an Alternating Magnetic Field. M.S. Thesis, The University of Utah, 1998.

47. Naidu, H. Electrodynamic Separation of Metallic Granules from Flowing Mixed Waste Stream. M.S. Thesis, University of Utah, 2010.

48. Saurabh, S. High Frequency Eddy Current Separation of Metallic Granules from Foundry Sand, E-scrap and Other Waste Streams. M.S Thesis, University of Utah, 2009.

49. Saurabh, S.; Rajamani, R. K. Eddy Current Separation of Metallic Granules from Waste Streams. In *Separation Technologies for Minerals, Coal, and Earth Resources*; SME: Denver, CO, 2012.

50. Landau, L. D.; Lifshitz, E. M. *Electrodynamics of Continuous Media*, 2nd ed.; Electrodynamics of Continuous Media; Pergamon Press: Oxford, UK, 1960.